Binding properties of the N-acetylglucosamine and high-mannose N-glycan PP2-A1 phloem lectin in Arabidopsis.

Julie Beneteau, Denis Renard, Laurent Marché, Elise Douville, Laurence Lavenant, Yvan Rahbé, Didier Dupont, Françoise Vilaine, Sylvie Dinant

Binding Properties of the *N*-Acetylglucosamine and High-Mannose *N*-Glycan PP2-A1 Phloem Lectin in Arabidopsis[W]

Julie Beneteau[1], Denis Renard, Laurent Marché, Elise Douville, Laurence Lavenant, Yvan Rahbé, Didier Dupont, Françoise Vilaine, and Sylvie Dinant*

UR1268 Unité de Recherches Biopolymères Interactions Assemblages, INRA, F–44300 Nantes, France (J.B., D.R., L.M., E.D., L.L.); Institut Jean Pierre Bourgin (J.B., F.V., S.D.) and Laboratoire Commun de Biochimie (F.V.), UMR 1318 INRA-AgroParisTech, INRA Centre de Versailles-Grignon, F–78000 Versailles, France; UMR 203 Laboratoire Biologie Fonctionnelle, Insectes et Interactions, INSA-NRA, F–69621 Villeurbanne, France (Y.R.); and UMR 1253 Sciences et Technologies du Lait et de l'Oeuf, INRA, F–35042 Rennes, France (D.D.)

Phloem Protein2 (PP2) is a component of the phloem protein bodies found in sieve elements. We describe here the lectin properties of the Arabidopsis (*Arabidopsis thaliana*) PP2-A1. Using a recombinant protein produced in *Escherichia coli*, we demonstrated binding to *N*-acetylglucosamine oligomers. Glycan array screening showed that PP2-A1 also bound to high-mannose *N*-glycans and 9-acyl-*N*-acetylneuraminic sialic acid. Fluorescence spectroscopy-based titration experiments revealed that PP2-A1 had two classes of binding site for *N*,*N*′,*N*″-triacetylchitotriose, a low-affinity site and a high-affinity site, promoting the formation of protein dimers. A search for structural similarities revealed that PP2-A1 aligned with the Cbm4 and Cbm22-2 carbohydrate-binding modules, leading to the prediction of a β-strand structure for its conserved domain. We investigated whether PP2-A1 interacted with phloem sap glycoproteins by first characterizing abundant Arabidopsis phloem sap proteins by liquid chromatography-tandem mass spectrometry. Then we demonstrated that PP2-A1 bound to several phloem sap proteins and that this binding was not completely abolished by glycosidase treatment. As many plant lectins have insecticidal activity, we also assessed the effect of PP2-A1 on weight gain and survival in aphids. Unlike other mannose-binding lectins, when added to an artificial diet, recombinant PP2-A1 had no insecticidal properties against *Acyrthosiphon pisum* and *Myzus persicae*. However, at mid-range concentrations, the protein affected weight gain in insect nymphs. These results indicate the presence in PP2-A1 of several carbohydrate-binding sites, with potentially different functions in the trafficking of endogenous proteins or in interactions with phloem-feeding insects.

The vascular tissues of land plants are responsible for the allocation of nutrients from their sites of uptake and synthesis. They also act as major routes for signaling between distant organs in response to biotic or abiotic stresses, physiological adjustments, and developmental switches. The phloem plays a major role in this long-distance signaling pathway by transporting a range of signal molecules, including hormones, metabolites, and macromolecules (Van Bel, 2003; Dinant et al., 2010). The phloem sap translocation stream involves highly specialized cells forming the sieve elements, which consist of enucleated cells with no known transcriptional or translational activity when fully differentiated (Sjölund, 1997). Most of the RNA and protein molecules found in sieve elements are thought to be transported from the neighboring companion cells through symplasmic connecting plasmodesmata (Lucas and Lee, 2004). Some of the proteins in the sieve element probably remain anchored to the parietal layers and help to maintain the cell machinery (Van Bel, 2003), but most macromolecules are transported by mass flow to distant organs, where they may have non-cell-autonomous effects on gene expression (Banerjee et al., 2004; Lough and Lucas, 2006; Corbesier et al., 2007). This model assumes the existence of an efficient delivery pathway between companion cells and sieve elements (Kim, 2005) and a regulatory trafficking control system for the long-distance targeting of macromolecules. A destination-selective mechanism was also proposed for the trafficking of proteins in sieve elements (Aoki et al., 2005). A few non-cell-autonomous proteins (NCAPs) binding to phloem sap proteins and acting as chaperones have been implicated in this long-distance trafficking pathway (Aoki et al., 2002, 2005; Lee et al., 2003; Taoka et al., 2007; Ham et al., 2009).

Despite the recent descriptions of large sets of macromolecules, including proteins, mRNAs, and small RNAs, in phloem sap (Kehr, 2006; Kehr and Buhtz, 2008; Dinant and Lemoine, 2010), our understanding of the mechanisms of transport of these

[1] Present address: Unité d'Ecologie et de Physiologie du Système Digestif, INRA Domaine de Vilvert, 78352 Jouy-en-Josas, France.

* Corresponding author; e-mail sylvie.dinant@versailles.inra.fr.

The author responsible for distribution of materials integral to the findings presented in this article in accordance with the policy described in the Instructions for Authors (www.plantphysiol.org) is: Sylvie Dinant (sylvie.dinant@versailles.inra.fr).

[W] The online version of this article contains Web-only data.
www.plantphysiol.org/cgi/doi/10.1104/pp.110.153882

molecules into and through sieve elements remains incomplete. Sieve elements have a unique cellular organization in which the plasma membrane and smooth parietal endoplasmic reticulum are retained but the other endomembrane systems, such as the Golgi apparatus, the tonoplast, and the nucleus, disappear during differentiation (Van Bel, 2003). There are also no organized microtubules and microfilaments (Evert, 1990). The trafficking of macromolecules, therefore, presumably depends on other as yet unidentified networks, regulating the entrance and exit of macromolecules and preventing the obstruction of sieve pores.

P-proteins (for phloem proteins) are idiosyncratic sieve element structures thought to be involved in regulatory processes within sieve elements. They are defined as large proteinaceous bodies observed on transmission electron microscopy and found in the sieve elements of dicotyledonous and many monocotyledonous species (Evert, 1990). Depending on the species and stage of development, P-proteins may be observed as filaments, tubules, or crystalline structures (Esau, 1969). It has been proposed that P-proteins are involved in defenses against pathogen colonization of the phloem or against sap-sucking insects, such as aphids. They are thought to occlude the sieve pores in case of injury (Spanner, 1978). Light and confocal laser scanning microscopy studies have demonstrated that forisomes, crystalloid P-proteins found in *Vicia faba* and other faboid legumes, control the conductivity of sieve tubes (Knoblauch et al., 2001, 2003). The components of the forisomes have been identified and appear to be proteins unique to faboid legumes, although some of the motifs they contain have been identified in proteins from other plant taxa (Noll et al., 2007; Pelissier et al., 2008). These findings demonstrate a role of forisome-type P-proteins in the occlusion of sieve tubes in the Fabaceae, but the function of the P-proteins present in other species remains unclear.

The composition of filamentous P-proteins has been determined in cucurbits, from which large amounts of phloem sap can be collected. In *Cucurbita maxima*, the P-proteins are the two most abundant sap proteins: Phloem Protein1 (PP1), which belongs to a gene family found only in cucurbits (Clark et al., 1997), and PP2, which belongs to a large gene family in angiosperms (Bostwick et al., 1992, 1994; Dinant et al., 2003). In cucurbits, PP2s display additional properties, including RNA binding (Gómez and Pallás, 2001, 2004; Owens et al., 2001; Gómez et al., 2005), trafficking from cell to cell, and modification of the size exclusion limit of the plasmodesmata (Balachandran et al., 1997). These observations suggest that PP2 might play a role in the cell-to-cell trafficking of macromolecules. In *C. maxima*, PP2 is produced in companion cells, but the protein accumulates in sieve elements (Dannenhoffer et al., 1997) and is transported across long distances (Golecki et al., 1998, 1999). Early studies suggested that the P-proteins of *C. maxima* exist in at least two structural states: large polymers immobilized in individual sieve elements, and small polymers or individual subunits translocated over long distances (Read and Northcote, 1983a). A phloem-specific pattern of expression has been reported for the *PP2* genes in two other plant species: *Apium graveolens* (*AgPP2-1*), a member of the Apiaceae, and Arabidopsis (*Arabidopsis thaliana*; *AtPP2-A1* and *AtPP2-A2*), a crucifer. In both species, these genes were found to be expressed specifically in the companion cell-sieve element complex (Dinant et al., 2003). PP2 transcripts have also been found in phloem transcriptomes from various species (Ivashikina et al., 2003; Vilaine et al., 2003; Schrader et al., 2004; Zhao et al., 2005; Le Hir et al., 2008) and more recently in the companion cell translatome in Arabidopsis (Mustroph et al., 2009).

The PP2s isolated from *C. maxima* and *Cucumis melo* have lectin activity (Sabnis and Hart, 1978; Allen, 1979; Read and Northcote, 1983b; Dinant et al., 2003). These proteins bind to chitin columns, demonstrating an affinity for oligomers of GlcNAc. These observations led Allen (1979) and Read and Northcote (1983a) to suggest a role in defenses against fungi or bacteria. Other lectins that bind to oligomers of GlcNAc have been identified in plants, and interactions with glycoproteins from plant pathogens, including fungi, have been demonstrated for some of these molecules (Peumans and Van Damme, 1995). Plant lectins also frequently display insecticidal activity (Carlini and Grossi-de-Sa, 2002; Vasconcelos and Oliveira, 2004). Furthermore, it has recently been suggested that carbohydrate-binding properties are involved in endogenous signaling processes (Van Damme et al., 2004), although little is known about the role of PP2 in the recognition of endogenous or foreign glycosylated molecules.

Despite the large body of information available, studies on the properties and functions of PP2 phloem lectins have been limited thus far to cucurbits. This is mainly because of the phloem properties of cucurbits, which exude large volumes of phloem sap (Turgeon and Wolf, 2009) and have higher concentrations of proteins in phloem sap, up to 100 mg mL^{-1} (Richardson et al., 1982), than the plants of other families (0.1–2.0 mg mL^{-1}; Thompson and Schulz, 1999). However, the composition of P-proteins and functions of PP2 proteins may differ in other species. Therefore, we investigated the properties of an Arabidopsis phloem PP2, PP2-A1. We produced large amounts of PP2-A1 protein in *Escherichia coli*, making it possible to analyze in detail the carbohydrate-binding properties of PP2-A1. We also investigated the binding of PP2-A1 to phloem sap proteins and its effect on aphids in an in vitro diet assay with the pea aphid *Acyrthosiphon pisum* (for which Arabidopsis is a nonhost species) and the green peach aphid *Myzus persicae* (for which Arabidopsis is a host species). The results of these experiments, together with those for intrinsic fluorescence spectroscopy and surface plasmon resonance, indicated that PP2-A1 contains several carbohydrate-binding sites with potentially different functions in the trafficking of endogenous proteins or interactions with sap-sucking insects.

RESULTS

Translational Fusion of PP2-A1 with a His_6 Tag

The *PP2-A1* gene (GenBank accession no. At4g19840.1) encodes a 246-amino acid protein (28.1 kD; accession no. O81865), as predicted from the identification of an open reading frame from the sequences of the *PP2-A1* cDNA (Dinant et al., 2003) and of full-length cDNAs available from GenBank (AY085730, AY090355, BX829358, AY122906, and BT015460). Arabidopsis produces only very small amounts of phloem sap by exudation (Barnes et al., 2004). Therefore, we generated recombinant PP2-A1 by heterologous expression in *E. coli*. This bacterium is a suitable host because there is no evidence that PP2 phloem lectins require glycosylation for activity in vivo (Allen, 1979; Balachandran et al., 1997). The *PP2-A1* cDNA was amplified from Arabidopsis total RNA, and the coding region was fused in frame with a 6× His tag (His_6) in the C-terminal position to facilitate its subsequent purification on a Ni^{2+}-nitriloacetic affinity column. This sequence was introduced into the *E. coli* expression vector pET9, for expression in the Tuner DE3 pLys S strain.

Production of Recombinant PP2-A1-His_6

The recombinant PP2-A1-His_6 was produced in *E. coli* grown in a large-scale fermentor. The protein was purified in a one-step process on a nickel affinity column. Recombinant PP2-A1-His_6 resolved as a doublet with an apparent molecular mass of about 28 kD on a denaturing gel (data not shown). Electrospray ionization-mass spectrometry (ESI-MS) data confirmed the presence of two polypeptides of 27.294 and 28.7895 kD (mass accuracy of 0.01%). These proteins had overlapping sequences, as confirmed by matrix-assisted laser desorption ionization (MALDI)-MS analysis after treatment with trypsin, and together they covered up to 67% of the PP2-A1 sequence. The two polypeptides differed only in terms of their N-terminal ends. The largest protein corresponded to the predicted PP2-A1 sequence (including a HCSELLPNK peptide corresponding to codons 5–12), whereas the shorter peptide lacked the first 13 N-terminal amino acids. This shorter product was the most abundant, and its sequence began just after a second in-frame Met initiation codon, located exactly 13 codons downstream from the predicted translation initiation codon (Supplemental Fig. S1). This observation is consistent with the new revised annotation (Alexandrov et al., 2006), which has reassigned the start codons of a number of Arabidopsis genes, including *PP2-A1*, based on a more favorable consensus sequence for the initiation of translation (accession no. AAM62948). The shorter product was consistent with a theoretical mass of 27.2964 kD after posttranslational removal of the N-terminal Met in *E. coli*. The mass of the larger product (28.7895 kD) was also consistent with the removal of the N-terminal Met in *E. coli* (theoretical mass of 28.7932 kD; Supplemental Fig. S1).

A second construct, based on the second initiation codon, with the coding sequence in translational fusion with a C-terminal His_6 tag, was generated to ensure that a homogeneous product was obtained. This second recombinant PP2-A1-His_6 was produced according to the same procedure. After purification, a single product was obtained with a mass of 27.4282 kD, as determined by MS, consistent with the theoretical molecular mass of 27.4276 kD. The two constructs yielded similar amounts of proteins (mean of 100 mg L^{-1}) with similar mobility on electrophoresis on denaturing gels (data not shown). The shorter version of the recombinant PP2-A1-His_6 was used in all the experiments described below, unless otherwise specified.

PP2-A1-His_6 Binds to a Chitin Column

A chitin column was used to determine the capacity of PP2-A1-His_6 to interact with oligomers of GlcNAc. This affinity column consisted of GlcNAc polymers. The recombinant PP2-A1-His_6 was produced in bacteria, and the crude bacterial extract was applied to a GlcNAc-Sepharose column. After elution, the various bound and unbound fractions were analyzed by SDS-PAGE (Fig. 1). Most bacterial proteins were not retained on the column after stringent elution in alkaline conditions. The main protein recovered was a 27.5-kD product with an electrophoretic mobility similar to that of the recombinant PP2-A1-His_6 purified on the nickel affinity column (Fig. 1, lane 8). The recombinant protein, therefore, had a strong capacity for binding oligomers of GlcNAc. The bound fraction yielded a second band of about 56 kD. This product may correspond to a dimer.

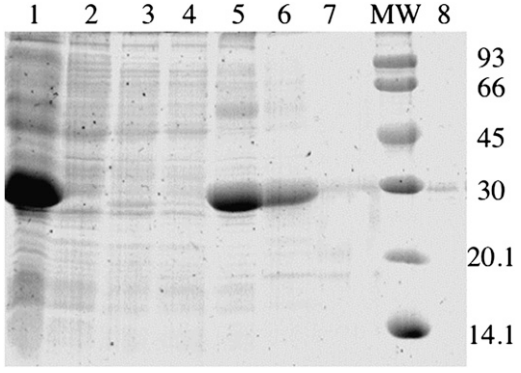

Figure 1. Binding of recombinant PP2-A1-His_6 to a chitin affinity column. SDS-PAGE on a 15% polyacrylamide gel of the various fractions obtained during purification on a chitin affinity column. Lane 1, Soluble fraction of the bacterial culture after PP2-A1-His_6 production in *E. coli*. Lane 2, Unbound fraction after column loading. Lanes 3 and 4, Fractions eluted after washing with extraction buffer (50 mM Tris and 200 mM NaCl, pH 8). Lanes 5 to 7, Fractions eluted from the column with successive NaOH treatments (0.05, 0.1, and 0.5 M NaOH); this elution revealed the main bound protein to be PP2-A1-His_6. Lane 8, For comparison, loading of 1 μg of purified recombinant PP2-A1-His_6 obtained after loading on a nickel affinity column. MW, Molecular weight marker.

PP2-A1-His$_6$ Binds to GlcNAc Oligomers, High-Man *N*-Glycans, and a Sialic Acid

We demonstrated specific binding of PP2-A1-His$_6$ using the glycan array developed by the Consortium for Functional Glycomics (www.functionalglycomics.org). Version 3.1 of this array, consisting of 377 different glycans, was used to determine the specificity and relative affinity of PP2-A1-His$_6$ for oligosaccharides (Blixt et al., 2004). In this assay, protein binding was quantified with a fluorescent antibody against the His$_6$ tag present on the recombinant protein. PP2-A1-His$_6$ was tested at several concentrations (0.1, 10, 50, and 100 μg mL^{-1}). At a concentration of 0.1 μg mL^{-1}, no specific interaction was observed. At concentrations of 10 and 50 μg mL^{-1}, the signal increased linearly with protein concentration, indicating the relative affinity of PP2-A1-His$_6$ for the various glycans. At a higher concentration (100 μg mL^{-1}), strong binding to a large number of glycans was observed, indicating saturation.

The nine glycans for which fluorescence was strongest (largest number of relative fluorescence units) at a concentration of 50 μg mL^{-1} are displayed in Figure 2. They were classified into three classes. Short oligomers of GlcNAc were recognized; PP2-A1 preferentially bound *N*-acetyl (Ac) chitotriose (GlcAc$_{\beta1\text{-}4}$GlcNAc$_{\beta1\text{-}4}$GlcNAc$_\beta$) and displayed moderate binding to N-Ac chitopentose (GlcNAc$_{\beta1\text{-}4}$)$_5$ and N-Ac chitohexose (GlcNAc$_{\beta1\text{-}4}$)$_6$. Monomers and dimers of GlcNAc were not recognized. Several high-Man *N*-glycans were also strongly recognized by PP2-A1-His$_6$. These molecules were essentially sugars with a common minimal structure, Man$_{\alpha1\text{-}3}$(Man$_{\alpha1\text{-}6}$)Man$_{\beta1\text{-}4}$GlcNAc$_{\beta1\text{-}4}$GlcNAc$_\beta$ (Man$_3$GlcNAc$_2$), associated with additional Man $\alpha3$ or $\alpha6$ linkages. PP2-A1-His$_6$ also bound to the sialic chain 9-acyl-*N*-acetylneuraminic acid (9AcNeu$_5$Ac), although neither Neu$_5$Ac nor other sialic acids present on the glycan array were recognized. Comparison of the binding responses at different

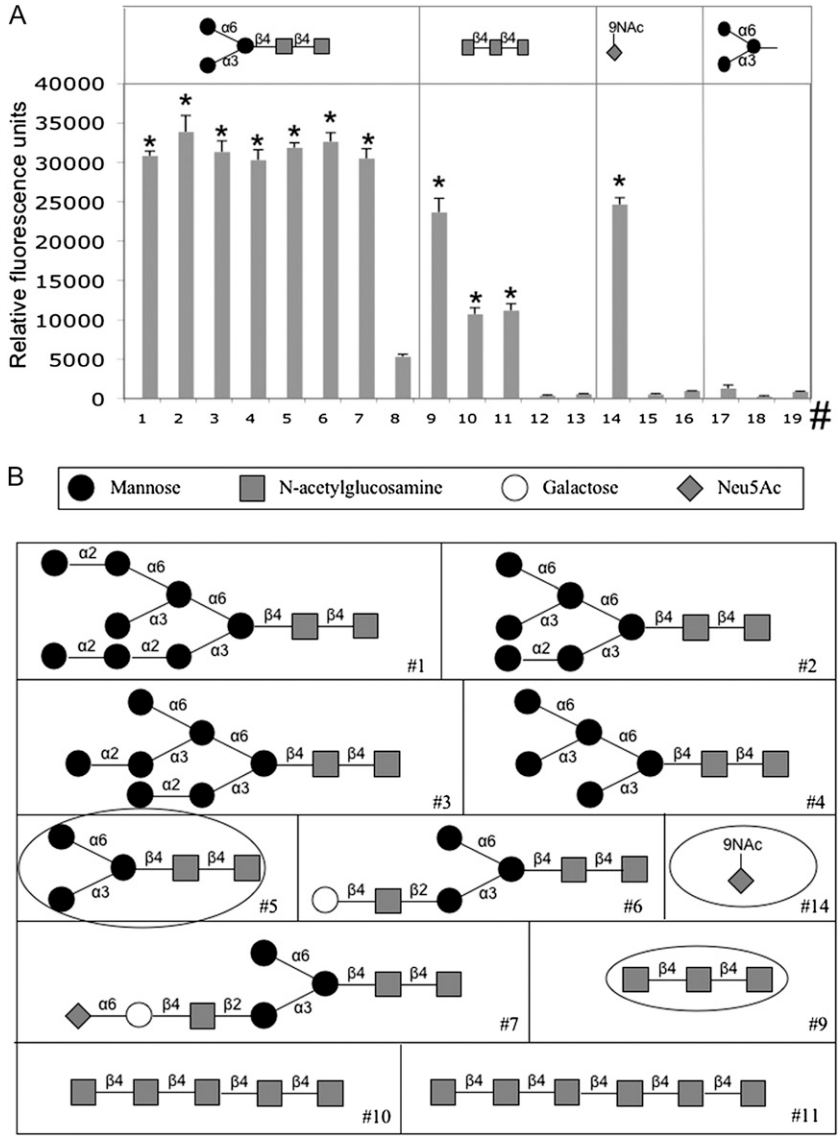

Figure 2. Spectrum of PP2-A1-His$_6$ lectin binding to the glycan microarray. A, Binding of PP2-A1-His$_6$ to glycans, expressed in relative fluorescence units of PP2-A1-His$_6$ (at a concentration of 50 μg mL^{-1}). The glycans giving the strongest signal (quantified in relative fluorescence units ± SE) are shown, as are several reference control sugars. The top panel shows the minimal glycan structure recognized for each glycan category. *, Glycans with a specific binding response ($P < 0.01$); #, numbers correspond to the name of the glycans (see below). B, Representation of the glycan structures displaying a specific response. Numbers correspond to the individual glycans, as indicated below. Man is represented by black circles, GlcNAc by gray squares, Gal by white circles, and Neu$_5$Ac by gray diamonds. PP2-A1-His$_6$ had the highest affinity for structures containing GlcNac$_{\beta1\text{-}4}$GlcNac$_{\beta1\text{-}4}$GlcNac$_{\beta1\text{-}4}$ and Man$_{\alpha1\text{-}3}$(Man$_{\alpha1\text{-}6}$)Man$_{\beta1\text{-}4}$GlcNAc$_{\beta1\text{-}4}$GlcNAc$_\beta$ (circled). PP2-A1-His$_6$ also displayed significant affinity for 9NacNeu$_5$Ac$_\alpha$. The names of the glycan structures represented are as follows: 1, Man$_{\alpha1\text{-}2}$Man$_{\alpha1\text{-}6}$(Man$_{\alpha1\text{-}3}$)Man$_{\alpha1\text{-}6}$(Man$_{\alpha2}$Man$_{\alpha2}$Man$_{\alpha1\text{-}3}$)Man$_{\beta1\text{-}4}$GlcNAc$_{\beta1\text{-}4}$GlcNAc$_\beta$; 2, Man$_{\alpha1\text{-}6}$(Man$_{\alpha1\text{-}3}$)Man$_{\alpha1\text{-}6}$(Man$_{\alpha2}$Man$_{\alpha1\text{-}3}$)Man$_{\beta1\text{-}4}$GlcNAc$_{\beta1\text{-}4}$GlcNAc$_\beta$; 3, Man$_{\alpha1\text{-}6}$(Man$_{\alpha1\text{-}2}$Man$_{\alpha1\text{-}3}$)Man$_{\alpha1\text{-}6}$(Man$_{\alpha2}$Man$_{\alpha1\text{-}3}$)Man$_{\beta1\text{-}4}$GlcNAc$_{\beta1\text{-}4}$GlcNAc$_\beta$; 4, Man$_{\alpha1\text{-}6}$(Man$_{\alpha1\text{-}3}$)Man$_{\alpha1\text{-}6}$(Man$_{\alpha1\text{-}3}$)Man$_{\beta1\text{-}4}$GlcNAc$_{\beta1\text{-}4}$GlcNAc$_\beta$; 5, Man$_{\alpha1\text{-}3}$(Man$_{\alpha1\text{-}6}$)Man$_{\beta1\text{-}4}$GlcNAc$_{\beta1\text{-}4}$GlcNAc$_\beta$; 6, Gal$_{\beta1\text{-}4}$GlcNAc$_{\beta1\text{-}2}$Man$_{\alpha1\text{-}3}$(Man$_{\alpha1\text{-}6}$)Man$_{\beta1\text{-}4}$GlcNAc$_{\beta1\text{-}4}$GlcNAc$_\beta$; 7, Neu$_5$Ac$_{\alpha2\text{-}6}$Gal$_{\beta1\text{-}4}$GlcNAc$_{\beta1\text{-}2}$Man$_{\alpha1\text{-}3}$(Man$_{\alpha1\text{-}6}$)Man$_{\beta1\text{-}4}$GlcNAc$_{\beta1\text{-}4}$GlcNAc; 8, GlcNAc$_{\beta1\text{-}2}$Man$_{\alpha1\text{-}3}$(GlcNAc$_{\beta1\text{-}2}$Man$_{\alpha1\text{-}6}$)Man$_{\beta1\text{-}4}$GlcNAc$_{\beta1\text{-}4}$(Fuc$_{\alpha1\text{-}6}$)GlcNAc$_\beta$; 9, GlcNAc$_{\beta1\text{-}4}$GlcNAc$_{\beta1\text{-}4}$GlcNAc$_\beta$; 10, (GlcNAc$_{\beta1\text{-}4}$)5$_\beta$; 11, (GlcNAc$_{\beta1\text{-}4}$)6$_\beta$; 12, GlcNAc$_{\beta1\text{-}4}$GlcNAc$_\beta$; 13, GlcNAc$_{\beta1\text{-}4}$; 14, 9NAcNeu$_5$Ac$_\alpha$; 15, 9NAcNeu$_5$Ac$_{\alpha2\text{-}6}$Gal$_{\beta1\text{-}4}$GlcNAc$_\beta$; 16, b-Neu$_5$Ac; 17, Man$_{\alpha1\text{-}3}$(Man$_{\alpha1\text{-}6}$)Man$_\alpha$; 18, Man$_{\alpha1\text{-}6}$Man$_\beta$; 19, Man$_{\beta1\text{-}4}$GlcNAc$_\beta$.

protein concentrations demonstrated that PP2-A1-His$_6$ had the highest affinity for high-Man *N*-glycans, oligomers of GlcNAc and 9AcNeu$_5$Ac (Fig. 3). No other glycans, including complex *N*-glycans or other *O*-linked glycans, were recognized (Supplemental Table S2). These findings provide evidence for the binding of PP2-A1-His$_6$ to glycans with different structures.

Surface Plasmon Resonance Analysis of Binding Properties

We studied the binding of PP2-A1-His$_6$ and *N*,*N*′,*N*″-triacetylchitotriose by surface plasmon resonance experiments assessing the capacity of PP2-A1-His$_6$ to interact with oligomers of GlcNAc. *N*,*N*′,*N*″-Triacetylchitotriose is a commercially available structural analog of chitotriose that is ideal for structural studies. The sensorgrams obtained after PP2-A1-His$_6$ immobilization on the CM5 sensorchip, with the analyte *N*,*N*′,*N*″-triacetylchitotriose circulating at different concentrations, are shown in Figure 4A. Differences in response between the response channel, where interaction took place, and the reference response channel, where no interaction occurred, were assessed as a function of time. We found that PP2-A1-His$_6$ readily bound *N*,*N*′,*N*″-triacetylchitotriose. The relative response, as a function of *N*,*N*′,*N*″-triacetylchitotriose concentration and displayed as lin-lin and log-log representations (Fig. 4B), reached a plateau at high sugar concentrations. Thus, all the binding sites were saturated for *N*,*N*′,*N*″-triacetylchitotriose concentrations exceeding 600 μg mL^{-1}. The response was not linear, and the curve did not have a sigmoid shape at higher sugar concentrations. These data are consistent with the involvement of several binding sites per molecule in the interaction of PP2-A1-His$_6$ with *N*,*N*′,*N*″-triacetylchitotriose. We analyzed the stoichiometry of the interaction by comparing the curve for the binding of *N*,*N*′,*N*″-triacetylchitotriose to immobilized PP2-A1-His$_6$ with the theoretical maximum binding capacity of the immobilized ligand (R_{max}). For a stoichiometry of 1:1, an R_{max} close to 45 resonance units (RU) was predicted. For concentrations of *N*,*N*′,*N*″-triacetylchitotriose greater than 400 μg mL^{-1}, we obtained values exceeding 45 RU, consistent with the binding of more than one molecule of *N*,*N*′,*N*″-triacetylchitotriose per molecule of PP2-A1-His$_6$. For a stoichiometry of 2:1, the predicted R_{max} value was about 90 RU. The experimental values obtained were slightly lower but were nonetheless best fitted by this model. These findings suggest that binding sites may not have been entirely accessible for interaction with *N*,*N*′,*N*″-triacetylchitotriose, because of the random orientation of the proteins after binding via amine coupling to carboxylmethyldextran.

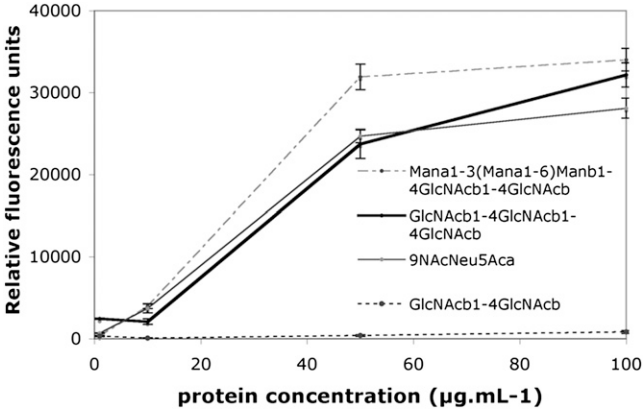

Figure 3. Relative affinity of the three main classes of oligosaccharides recognized by PP2-A1-His$_6$. Responses are in relative fluorescence units of the three minimal glycan skeletons for which PP2-A1-His$_6$ had the highest affinity at the various protein concentrations tested (0.1, 1, 10, 50, and 100 μg mL^{-1}). Error bars indicate SE; $n = 6$. Man$_{\alpha1\text{-}3}$(Man$_{\alpha1\text{-}6}$)Man$_{\beta1\text{-}4}$GlcNAc$_{\beta1\text{-}4}$GlcNAc is represented by a discontinuous gray line, GlcNAc$_{\beta1\text{-}4}$GlcNAc$_{\beta1\text{-}4}$GlcNAc$_{\beta}$ by a black line, and 9NAcNeu$_5$Ac by a solid gray line. These three glycans present a highly specific binding response (*t* test, $P < 0.01$) at concentrations of 10, 50, and 100 μg mL^{-1}. For comparison, GlcNAc$_{\beta1\text{-}4}$GlcNAc$_{\beta1\text{-}4}$, which is poorly recognized by PP2-A1-His$_6$, is also represented on the diagram.

Assessment of Binding Site Characteristics by Intrinsic Fluorescence Spectroscopy

Binding properties were further assessed by titration experiments using intrinsic fluorescence spectroscopy. The binding of *N*,*N*′,*N*″-triacetylchitotriose to PP2-A1-His$_6$ reduced Trp fluorescence intensity without changing the maximum emission wavelength, which remained at 344 nm (Fig. 5A). This quenching of Trp fluorescence probably reveals a slight change in the conformation of PP2-A1-His$_6$ following interaction with sugar moieties. The absence of a change in maximum fluorescence emission wavelength suggests that Trp residues may not be fully exposed to aqueous solvent, as reported previously in other binding systems (Renard et al., 1998). A hyperbolic fluorescence titration curve was obtained when the results were plotted as a function of sugar-protein molar ratio (Fig. 5B). The dissociation constant (K_d) and the number of sugar binding sites (n) were determined by fitting a Scatchard equation to the experimental curve, assuming a noncooperative model with independent and nonidentical sites (Fig. 5C). The K_d (slope) and n (intercept) values obtained from linear regression analysis suggested that *N*,*N*′,*N*″-triacetylchitotriose bound PP2-A1-His$_6$ through two different types of site: a high-affinity site with a K_d of 3.4×10^{-7} M and an n value of 0.5, and a low-affinity site with a K_d of 1.3×10^{-5} M and an n value of 1.9. These values for the number of binding sites suggest that two proteins (i.e. a dimer) bind one sugar via the high-affinity sites, whereas two sugars bind one protein via the low-affinity sites. The existence of two classes of site on PP2-A1 suggested that the interaction of *N*,*N*′,*N*″-triacetylchitotriose with PP2-A1 promoted the formation of a protein dimer (n = 0.5), with additional sugar molecules loosely binding to other regions of PP2-A1 (n = 1.9). Given the high affinity of the binding site

promoting the dimer formation, PP2-A1-His_6 probably exists as dimers or oligomers in solution.

Prediction of the Structure of the Carbohydrate-Binding Domain

Searches of the Pfam$^{\alpha 2-}$ and Prosite motif servers detected no lectin motifs in PP2-A1 or other related PP2s (CbmPP2, CmmLec17, and CmmLec26). Therefore, we tried to identify structural similarities to proteins of known structure, by BLAST searches, using PP2-A1 as the query and the CBS@tome2 metaserver against protein structure databases. PP2-A1 presented significant structural similarities (TITO scores < -60) to two classes of carbohydrate-binding modules (CBMs), the Cbm4 of the laminarase 16a (lam16a) from *Thermotoga maritima* and the Cbm22-2 of the

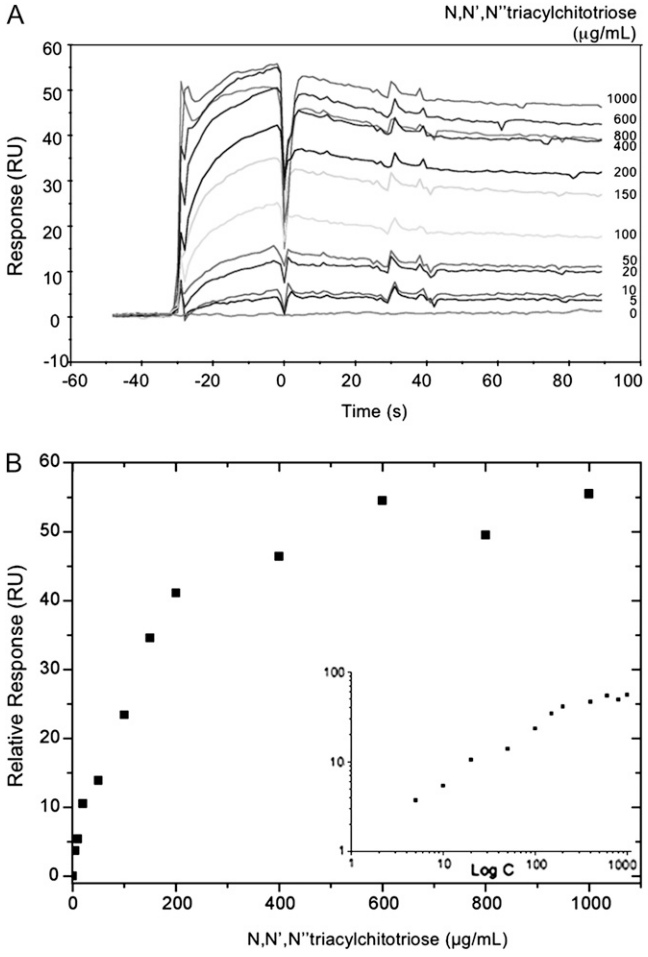

Figure 4. Surface plasmon resonance analysis of the properties of PP2-A1 binding to chitotriose. A, Sensorgrams of CM5 surface (response expressed in RU)-immobilized PP2-A1-His_6 with *N,N′,N″*-triacetylchitotriose injected at various concentrations (0, 5, 10, 20, 50, 100, 150, 200, 400, 600, 800, and 1,000 μg mL^{-1}). Sensorgrams were obtained in triplicate and were highly reproducible. B, Plots of relative response (maximal response obtained for each concentration, expressed in RU) as a function of *N,N′,N″*-triacetylchitotriose concentration (μg mL^{-1}) on lin-lin and log-log representations.

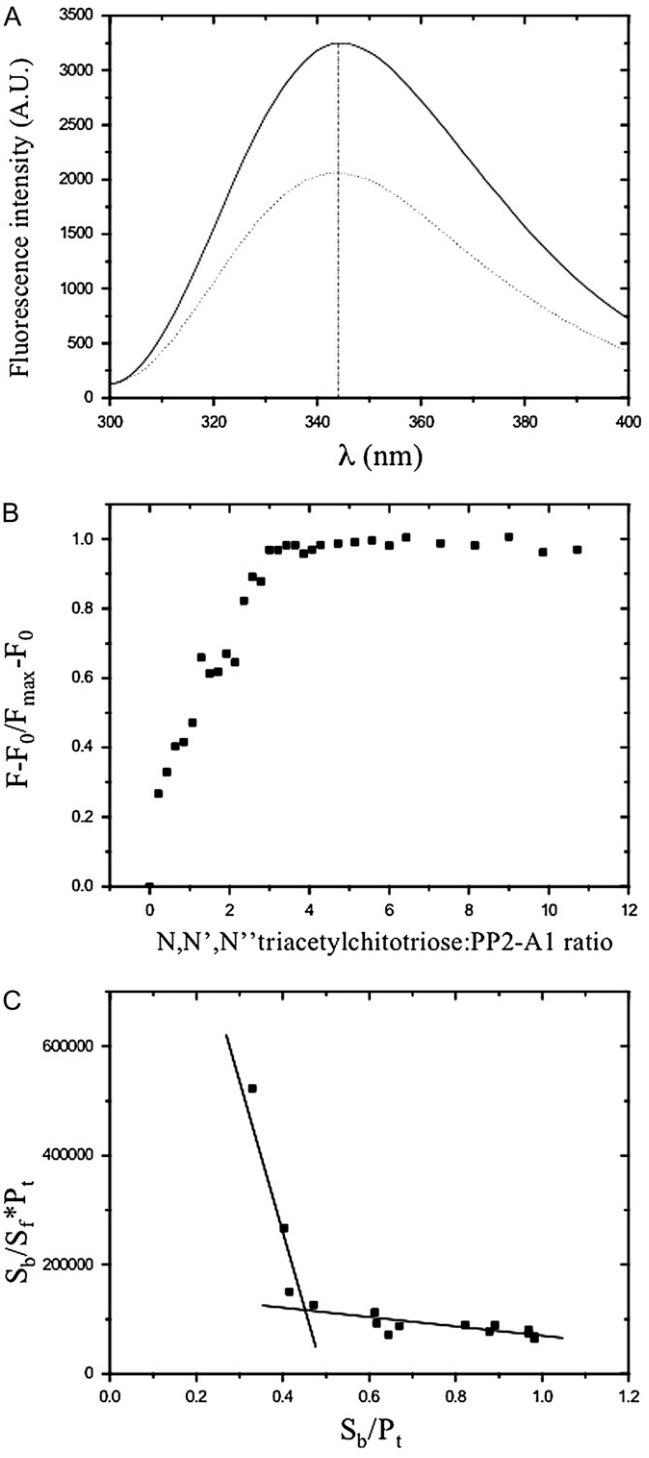

Figure 5. Analysis of the fluorescence spectrum of PP2-A1 in the presence of chitotriose. A, Fluorescence spectra of PP2-A1-His_6 alone (solid line) and PP2-A1-His_6 with *N,N′,N″*-triacetylchitotriose (dotted line; molar ratio 10.7) in universal buffer, pH 8. The wavelength of maximum fluorescence emission is indicated by the vertical dotted line. Spectra were recorded in duplicate and were reproducible. B, Curve for the titration of PP2-A1-His_6 with *N,N′,N″*-triacetylchitotriose. C, Scatchard plot of the data displayed in B with the fitting of a linear regression line. See text for explanations.

endo-1,4-β-xylanase Y (Xyn10B) from *Clostridium thermocellum*. These domains had a β-strand structure (Xie et al., 2001; Boraston et al., 2002) typical of carbohydrate-binding domains. In Cbm4 and Cbm22-2, the carbohydrate-binding site is located within a groove, in a structure consisting of parallel and antiparallel β-strands. Alignments of the sequences of PP2-A1 and of these CBM domains identified an overlap in the area corresponding to the structural β-strands. In PP2-A1, structural similarities were found in the sequence from residues 112 to 249, making up part of the conserved core of the protein, including part of domain A and domains B to D (Dinant et al., 2003). Based on the similarity to Cbm4, which gave the best consensus evaluation with the TITO program, a model for the structure of PP2-A1 was proposed (Fig. 6). In this model, the β-strands were positioned on the conserved core and constituted a pocket-like structure consisting of parallel or antiparallel β-strands. This region of similarity to CBM may be the putative lectin-binding site. Unlike lam16a and Xyn10B, PP2-A1 had no recognizable calcium-binding domain (data not shown). Structural predictions were not possible for the N-terminal region of PP2-A1 (residues 1–111).

PP2-A1-His$_6$ Binds to Phloem Sap Proteins

As PP2-A1 was potentially present in the phloem sap, we investigated the binding of PP2-A1-His$_6$ to phloem sap proteins. Phloem sap was obtained from mature rosette leaves with an EDTA-facilitated exudation technique (King and Zeevaart, 1974) adapted for Arabidopsis. The quality of the sap was confirmed by the smaller proportions of Glc and hexose than of Suc (Fig. 7A), as expected for phloem sap exudate. In addition, the phloem sap protein profile was clearly different from the profile for total proteins extracted from the leaf veins (Fig. 7B), further indicating low levels of contamination from other tissues. On SDS-PAGE, major bands were observed at 27 and 55 kD. These fractions were isolated from excised bands and analyzed for the characterization of abundant sap proteins. The proteins were analyzed by liquid chromatography-tandem mass spectrometry (LC-MS/MS). We unambiguously identified 24 proteins. The 27-kD fraction was significantly enriched in various isoforms of glutathione *S*-transferase and dehydroascorbate reductase (Supplemental Table S3). The 55-kD fraction was enriched in catalase, enolase phosphopyruvate hydratase, adenosylhomocysteinases, lipoamide dehydrogenase, and several Leu-rich repeat (LRR) proteins. Three proteins matched phloem sap proteins previously identified in phloem sap from a related species, *Brassica napus* (Giavalisco et al., 2006): the glutathione *S*-transferase GSTF9, the adenosylhomocysteinase HOG1, and the UDP-Glc pyrophosphorylase UGP2. In addition, we found peptides covering the elongation factor 2 LOS1 and the elongation factor α1 MUF9.8 also reported in the phloem sap of *B. napus* (data not shown). As this analysis covered only the 27- and 55-kD fractions, it probably covered only a fraction of the phloem sap proteome, overlapping only partially with the proteomes of other species, such as *B. napus*. PP2-A1 was not found in these fractions, although 27 and 55 kD are close to the theoretical masses for PP2-A1 monomers and dimers, respectively.

Far-western analysis was performed to determine whether PP2-A1-His$_6$ interacted with phloem sap proteins. PP2-A1-His$_6$ bound several sap proteins (Fig. 7C,

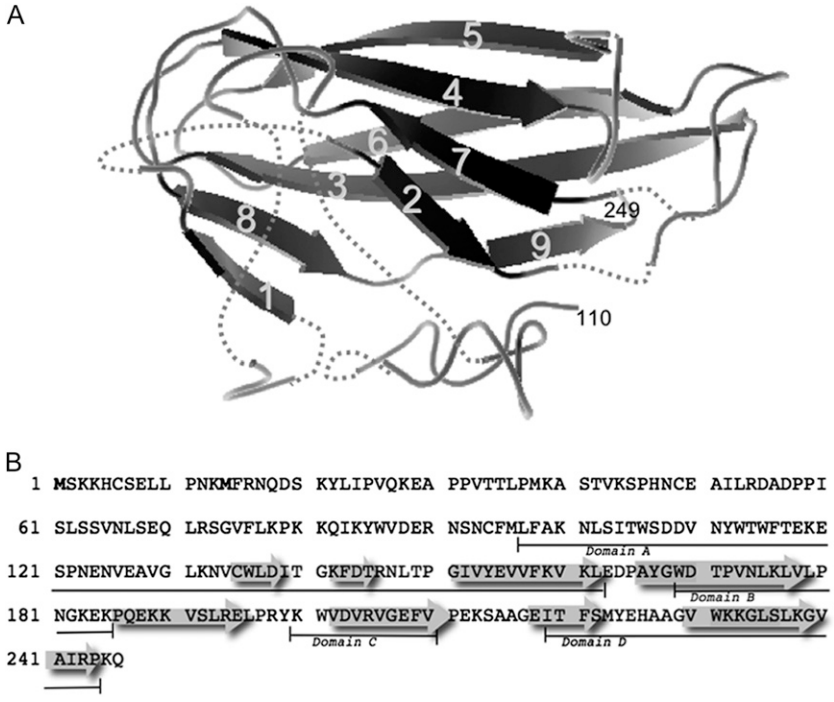

Figure 6. Hypothetical model of the tertiary structure of PP2-A1. This model presents a predicted carbohydrate-binding domain of PP2-A1 consisting of parallel and antiparallel β-strands, based on structural similarities with known CBMs. A, The positions of secondary structure elements for PP2-A1 are indicated on a ribbon representation from residues 110 to 249: β-strand 1 (136–139), β-strand 2 (143–146), β-strand 3 (152–163), β-strand 4 (167–179), β-strand 5 (187–194), β-strand 6 (203–211), β-strand 7 (219–223), β-strand 8 (231–239), and β-strand 9 (242–245). Loops (solid lines) and strands (arrows) were predicted by alignment with CBM4 and CBM22. Regions for which the alignments provided no appropriate prediction are indicated by dotted lines. B, Positions of conserved domains: domain A (97–162), domain B (169–186), domain C (196–210), and domain D (219–244).

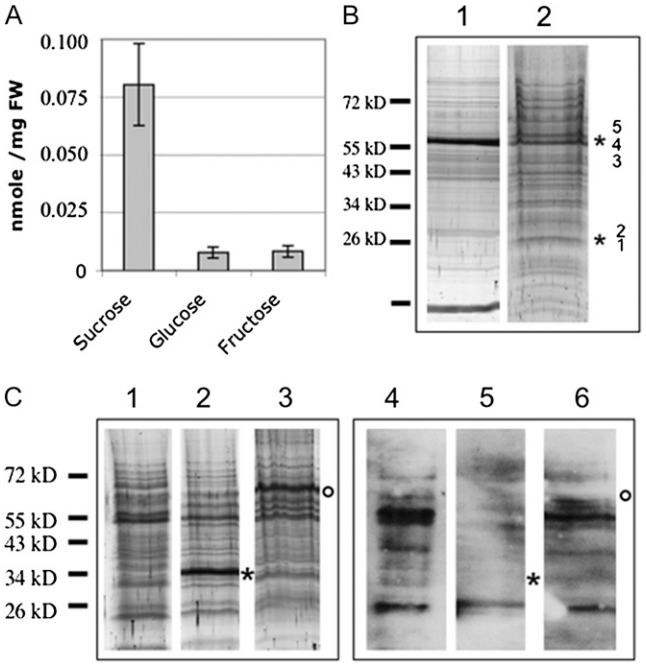

Figure 7. Analysis of the binding of PP2-A1 to phloem sap proteins. A, Sugar content of phloem sap exudate (nmol mg^{-1} fresh weight [FW]). Error bars indicate SE; $n = 6$. B, SDS-PAGE analysis (12% polyacrylamide gel) of phloem sap exudate (lane 2), including comparison with the total protein extracted from leaf veins (lane 1). The asterisk and numbers (1–5) in lane 2 indicate the various 26- and 52-kD fractions collected for LC-MS/MS analysis (fractions 1–5, as reported in Supplemental Table S3). For more details, see Supplemental Table S3. C, SDS-PAGE analysis (12% polyacrylamide gel) of phloem sap exudate before treatment (lanes 1 and 4) and after treatment with PNGase (lanes 2 and 5) or GDase (lanes 3 and 6). The migration of PNGase is indicated by asterisks and that of GDase by circles. Proteins were detected by staining (lanes 1–3) or by protein overlay using PP2-A1-His_6 and peroxidase-conjugated anti-His_6 antibody (lanes 4–6).

lane 4). At least 12 bands were revealed by protein overlay with PP2-A1-His_6. The most intense bands corresponded to proteins with apparent molecular masses of approximately 24 to 26, 43, and 55 to 60 kD. After glycosidase treatment to remove *N*-linked glycans (PNGase) or tGlcNAc (GDase; Fig. 7C, lanes 5 and 6, respectively), PP2-A1-His_6 still bound to phloem sap proteins, although closer examination revealed slight modifications to the binding pattern. PNGase treatment decreased the intensity of labeling of bands in the 24- to 26-kD and 55- to 60-kD fractions. Some bands in the 55- to 60-kD fraction were less strongly labeled after GDase treatment. Thus, although glycosidase treatments slightly altered the binding spectra of PP2-A1-His_6, they did not abolish its binding to phloem sap proteins.

Effect of PP2-A1-His_6 on the Growth of Aphids

The effect of PP2-A1-His_6 on insect weight gain and survival was assessed in an insect feeding bioassay. This experiment was conducted either with the pea aphid *A. pisum*, used as a reference aphid for lectin toxicity tests (Rahbé and Febvay, 1993), or with the green peach aphid *M. persicae*, an aphid infesting Arabidopsis. Aphid nymphal weight and mortality were assessed after the neonates fed for 7 d on an artificial diet supplemented with various concentrations of recombinant PP2-A1-His_6. Wheat germ agglutinin (WGA), a GlcNac lectin of limited toxicity to aphids (Rahbé and Febvay, 1993), and casein, a protein with no aphid toxicity, were used as controls in this experiment.

After 7 d, no significant difference in survival was observed between *A. pisum* and *M. persicae* nymphs fed on the control diet and nymphs fed on the diet supplemented with recombinant protein, regardless of the concentration of recombinant protein added to the medium (Supplemental Table S4). However, aphid weight was reduced at protein concentrations between 125 and 250 $\mu g\ mL^{-1}$ for *A. pisum* ($P < 0.001$ and $P = 0.0005$ for 125 and 250 $\mu g\ mL^{-1}$, respectively; Fig. 8) and between 83 and 250 $\mu g\ mL^{-1}$ for *M. persicae*, with the L06 clone ($P < 0.003$ for first biological replicate 1 and $P = 0.01$ for second replicate; Fig. 8). Similar results were obtained on a second clone of *M. persicae*, the LC05 clone (Supplemental Fig. S6). The loss of weight was more pronounced in *A. pisum* (33% maximal weight decrease) than in *M. persicae* (10%–20% maximum weight decrease). At higher concentrations (500–1,000 $\mu g\ mL^{-1}$), weight gain was unaffected in both *A. pisum* and *M. persicae*. No effect on the weight and survival of either aphid species was observed with WGA and casein (Fig. 8C).

In this bioassay, the recombinant protein had no effect on nymphal settlement in *A. pisum* or *M. persicae*, which was similar after 24 h on artificial diets with or without recombinant protein supplementation for all doses (Supplemental Table S4). This demonstrates that the recombinant protein had no deterrent effect in a no-choice assay. Similarly, in a choice assay in which the recombinant protein was present at a concentration of 200 $\mu g\ mL^{-1}$, there was no phagodeterrent effect after 16 h, either in *A. pisum* or in *M. persicae* (Supplemental Table S5), showing that the effect on weight gain did not result in changes in insect behavior. In such a choice test with the artificial diet supplemented with 500 $\mu g\ mL^{-1}$ recombinant protein, we observed a significant "deterrent" effect after 16 h with *A. pisum* ($P = 0.0004$), characterized by a negative phagostimulation index ($Ix = -0.53$; i.e. approximately 23% of aphids feed on the medium supplemented with PP2-A1-His_6). However, no effect was observed with either of the two clones of *M. persicae* used (Supplemental Table S5).

DISCUSSION

The phloem constitutes a strategic checkpoint for the mounting of defenses against pathogens and pests (van Bel and Gaupels, 2004). It provides an efficient pathway for long-distance communication and the

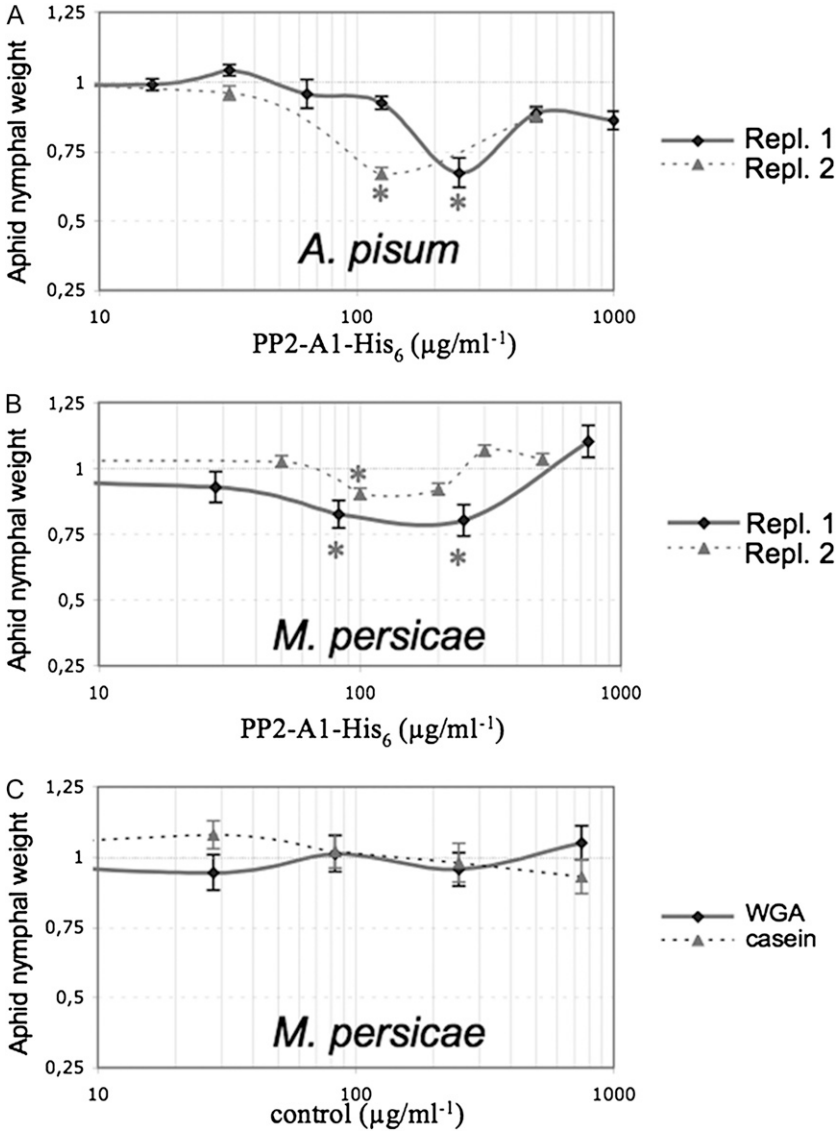

Figure 8. Effect of PP2-A1-His$_6$ on the growth of the aphids *A. pisum* and *M. persicae*. A, Growth of neonate nymphs of *A. pisum* after feeding for 7 d on an artificial diet containing various concentrations of PP2-A1-His$_6$ in two independent biological replicates (Repl.1 and Repl.2). Values are expressed as fractions of the mean weight for aphids fed on medium with and without recombinant protein. Error bars indicate SE. Aphid nymph $n > 30$. For all graphs, means differing from the control at a 5% risk level are indicated by asterisks (Dunnet's test). B, Growth of neonate nymphs of *M. persicae* (clone L06) after feeding for 7 d on an artificial diet containing various concentrations of PP2-A1-His$_6$. Two independent biological replicates were realized (Repl.1 and Repl.2). Values are expressed as fractions of the mean weight for aphids fed on medium with and without recombinant protein. Error bars indicate SE. Aphid nymph $n > 30$. A two-way ANOVA on standardized weight data (percentage of control) showed no clone effect ($P = 0.986$), no interaction ($P = 0.806$), and a significant dose effect ($P < 0.0001$); asterisks indicate means significantly different from control (Dunnet's test). C, Growth of neonate nymphs of *M. persicae* after feeding for 7 d on an artificial diet containing various concentrations of casein or WGA used as a negative control (casein) or a GlcNAc lectin control (WGA) with limited toxicity. Values are expressed as fractions of the mean weight for aphids fed on medium with and without protein. Error bars indicate SE. Aphid nymph $n > 18$. No effect of control proteins was detected ($P = 0.54$ for casein and $P = 0.44$ for WGA by ANOVA).

trafficking of macromolecules, although our knowledge of the phloem proteins involved in these processes remains incomplete (Lough and Lucas, 2006). PP2s constitute an interesting family of phloem proteins. They were first identified as components of the so-called P-proteins in cucurbits and shown to act as dimeric chitin-binding lectins in these plants (Beyenbach et al., 1974; Sabnis and Hart, 1978; Allen, 1979; Read and Northcote, 1983a; Smith et al., 1987; Bostwick et al., 1992), leading to the suggestion of a role in defense mechanisms. In *C. maxima*, CbmPP2 presents several properties associated with NCAPs (Bostwick et al., 1994; Balachandran et al., 1997; Golecki et al., 1998, 1999), suggesting a role in the trafficking of macromolecules. However, it remains unclear whether PP2s from species other than cucurbits present such properties. We demonstrated that lectin activity is conserved in Arabidopsis for the closest ortholog, PP2-A1. We then extended these results by characterizing the spectrum of sugar recognition, the properties of the binding sites, and by demonstrating binding to several phloem sap proteins. In addition, we propose a model for the structure of PP2-A1 based on structural predictions.

Structure Prediction

The PP2 family is unique to plants and is unrelated to other classes of plant lectins. Structural database searches revealed similarity to two CBMs comprising the catalytic domain of two bacterial enzymes involved in glycan modifications. The PP2-A1 region that aligned with the CBM pocket for sugar binding (Fig. 6) is predicted to fold into a parallel and antiparallel β-strand structure. This region overlaps the conserved region (residues 112–246), which includes part of domain A and the domains B to D (Dinant et al., 2003). It is unknown whether this predicted CBM

corresponds to the domain required for the lectin activity associated with PP2-A1. However, all the lectin domains crystallized to date have a structure based on β-strands, supporting the hypothesis that the domain predicted to fold into β-strands in PP2-A1 may be responsible for its lectin activity. It was not possible to assign a structure to the first 111 N-terminal residues of the protein. This N-terminal region contains no known motif. However, other PP2 proteins have an extension at their N termini, often containing protein-protein interaction motifs, such as the F-box, TOLL domain, or AIG1 domain (Dinant et al., 2003). Thus, despite the absence of any known domain in PP2-A1, this region may also contain a binding domain that has yet to be identified.

PP2-A1 Is a GlcNAc Oligomer-Binding Lectin with Two Types of Binding Site

The chitin-binding assay showed that PP2-A1-His_6 produced in *E. coli* bound GlcNAc oligomers (Fig. 1), as reported for the cucurbit PP2 phloem lectins. Glycan array screening further extended these results by showing that PP2-A1-His_6 preferentially recognized $(GlcNAc)_3$ chitotriose and had a lower affinity for $(GlcNAc)_5$ and $(GlcNAc)_6$ oligomers. No recognition was observed for GlcNAc dimers and monomers (Fig. 2). The specificity of the interaction with $(GlcNAc)_3$ chitotriose was confirmed by surface plasmon resonance analysis (Fig. 4) and characterized further by intrinsic fluorescence spectroscopy based on titration with *N*,*N*′,*N*′′-triacetylchitotriose (Fig. 5). We identified two classes of binding site. Each PP2-A1 dimer had one high-affinity binding site ($K_d = 3.4 \times 10^{-7}$ M, $n = 0.5$) and each monomer had two low-affinity sites ($K_d = 1.3 \times 10^{-5}$ M, $n = 1.89$). This result is important, as it demonstrates that sugar binding is closely connected to dimer formation.

PP2 lectins from cucurbits and the related protein Nictaba have been reported to be dimeric in planta (Read and Northcote, 1983a; Chen et al., 2002; Walz et al., 2004). The existence of a high-affinity site in PP2-A1 dimeric forms is consistent with these observations. However, it remains unclear whether dimer formation is a prerequisite for the binding of sugar moieties or whether sugars are required for the formation of dimeric PP2-A1. The binding of PP2-A1 to other sugars (see below) probably renders the system even more complex, because these sugars may also have different affinities for PP2-A1 subunits and dimers. This raises the question of the conditions required for oligomerization in vivo and the role of PP2 subunits and aggregates in planta, as previously considered for the cucurbit PP1 and PP2 phloem proteins (Read and Northcote, 1983a; Leineweber et al., 2000).

PP2-A1 Binds to Different Classes of Glycans

Glycan array screening revealed that, in addition to GlcNAc oligomers, PP2-A1-His_6 bound to high-Man *N*-linked glycans and to a sialic acid derivative (Fig. 2). This extends the specificity of the phloem PP2-A1 lectin to previously unsuspected classes of glycans. PP2-A1-His_6 bound $9NAcNeu_5Ac$ with high affinity. Sialic acids are present neither in plants nor in their pathogens, although a few sialic acid-specific plant lectins are known (Lehmann et al., 2006; Zeleny et al., 2006). Sialylation occurs mostly in mammals, birds, and their pathogenic microorganisms, in which it acts in recognition phenomena (Vimr and Lichtensteiger, 2002; Schauer, 2009). The recognition of $9NAcNeu_5Ac$ by PP2-A1 may thus facilitate binding to sialylated proteins from animal herbivores, as suggested for other plant lectins from this group (Lehmann et al., 2006).

PP2-A1-His_6 also bound high-Man *N*-linked glycans, with a common $Man_3GlcNAc_2$ core structure, which was recognized with high affinity (Fig. 3). High-Man *N*-glycans are found in animals, plants, plant pathogens, and insects. High-Man *N*-glycans are processed in the endoplasmic reticulum (Lerouge et al., 1998). In plant cells, oligomannoside glycans account for only a small fraction of *N*-glycans and $Man_3GlcNAc_2$ is rare (Strasser et al., 2004, 2005). The secretory pathway of sieve elements is limited (Van Bel, 2003), potentially limiting the formation of complex glycans and leading to an enrichment in glycoproteins with high-Man *N*-glycans. It is possible, therefore, that PP2-A1-His_6 recognizes phloem sap glycoprotein. $Man_3GlcNAc_2$ is also the major processed *N*-glycan produced by insect cells (Hollister et al., 2002; Tomiya et al., 2004); insects are thus an obvious potential target (see below).

Based on our glycan array analysis, it now appears that PP2-A1-His_6 binds different classes of glycans. This result raises the interesting possibility that the phloem PP2 lectin plays several roles, recognizing either endogenous glycoproteins or glycosylated receptors of pathogens and herbivores feeding on phloem sap.

A Role for PP2-A1 in the Recognition of Phloem Sap *O*-GlcNAc Proteins?

The binding of PP2-A1-His_6 to small oligomers of GlcNAc is consistent with previous reports for other PP2 lectins (Sabnis and Hart, 1978; Allen, 1979). PP2-A1-His_6 did not bind to long GlcNAc oligomers and therefore is unlikely to be involved in recognizing the chitin found in insects and fungi. Instead, it may be involved in the recognition of *O*-linked GlcNAc, such glycans being found in glycoproteins from many organisms. Terminal GlcNAc are found as monomers in animal cells (Hanover, 2001; Wells and Hart, 2003) and as oligomers in plant cells (Heese-Peck et al., 1995). GlcNAc glycosylation occurs in the cytoplasm and is involved in various signaling pathways and nucleocytoplasmic cycling (Hart et al., 2007). Phloem sap and plant viral proteins can be modified by *O*-GlcNAc glycosylation (Chen et al., 2005; de Jesus Perez et al.,

2006; Scott et al., 2006; Taoka et al., 2007). Non-cell-autonomous pathway protein 1, which is required for the trafficking of glycosylated proteins through plasmodesmata (Taoka et al., 2007), binds *O*-GlcNAc proteins in phloem sap. The phloem Hsp70 is another candidate protein for binding to *O*-GlcNAc phloem sap proteins (Aoki et al., 2002). These studies led the authors to propose that transport, through plasmodesmata, between companion cells and sieve elements, like shuttling between the nucleus and the cytoplasm, involves *O*-GlcNAc glycosylation.

Based on our current findings, we suggest that PP2-A1 may bind *O*-GlcNac proteins. We established that PP2-A1-His$_6$ bound to phloem sap proteins based on the observation that PP2-A1-His$_6$ interacted with several proteins, ranging from 20 to 80 kD in size (Fig. 7). Moreover, our results indicate that the range of PP2-A1-His$_6$ protein binding is broader than previously found, for example in *C. maxima*, in which PP2 was shown to interact only with PP1 (Read and Northcote, 1983a, 1983b). The binding of PP2-A1-His$_6$ to phloem sap proteins was not entirely abolished by treatment with GDase (removing GlcNAc glycans) or PNGase (removing *N*-glycans), demonstrating that recognition does not strictly depend upon glycosylation. Such interactions may be involved in a range of processes, such as interaction with phloem sap proteins for their entry into the sieve elements, long-distance trafficking, signal transduction, or folding. The recent observation that PP2-A1 enhances the transmission of a plant virus by aphids and stabilizes virus particles in vitro (Bencharki et al., 2010) is consistent with a role as a chaperone. PP2 is abundant in the phloem and is transported from companion cells to sieve elements. Therefore, it would be abundant enough to chaperone the trafficking of glycoproteins from the companion cells to the sieve elements, although additional investigations in vivo are required to confirm a number of hypotheses.

A Role for PP2-A1 in the Plant-Aphid Interaction?

Plant lectins are often insecticidal, as illustrated by the Man-binding lectins, which act by binding to the glycoproteins of midgut epithelial cells (Vasconcelos and Oliveira, 2004). As the PP2-A1-His$_6$ protein bound to three classes of glycans, including $Man_3GlcNAc_2$, a major glycan in insect cells, we investigated the insecticidal effects of PP2-A1 on aphid feeding. Two species were tested: *A. pisum*, which is a model species for lectin toxicity (Rahbé and Febvay, 1993), and *M. persicae*, for which Arabidopsis is a common host. For this assay, we used a range of protein concentrations, from 16 to 1,000 μg mL^{-1}. Nothing is known about the concentration of phloem sap proteins in Arabidopsis and most other species. In rice (*Oryza sativa*), the concentrations of abundant proteins have been estimated at about 10 μg mL^{-1} (Suzui et al., 2006) and those of total soluble proteins have been estimated at about 150 to 200 μg mL^{-1} (Hayashi et al., 2000). Local concentrations of PP2-A1 in phloem sap are probably not homogeneous, because of local self-assembly. Therefore, it remains unclear whether the range of concentrations used in the artificial aphid bioassay, which are standard for toxicity tests, overlaps with local concentrations of PP2 in phloem sap.

When added to an artificial aphid diet at concentrations of 125 to 250 μg mL^{-1} depending on the assay, PP2-A1-His$_6$ had a slightly detrimental effect on the weight gain of *A. pisum* nymphs (Fig. 8A), which were up to 30% lighter than the controls after 7 d of feeding. A similar effect was observed on *M. persicae* nymphs, with 83 to 250 μg mL^{-1} recombinant protein, although more moderate (nymphs 10%–20% lighter; Fig. 8B). In this no-choice test, aphid settlement and survival were not affected, demonstrating that PP2-A1-His$_6$ was not acutely toxic at this range of concentrations (Supplemental Table S4). Similarly, at a concentration of 200 μg mL^{-1}, no deterrent effect on any aphid species was detected in a choice assay (Supplemental Table S5). Thus, the slight growth-inhibitory effect was probably not due to a preingestion effect. The smaller weight gain may instead result from the modulation of ingestion, with the presence of PP2-A1-His$_6$ in food preventing aphids from feeding abundantly. Alternatively, PP2-A1-His$_6$ may limit the aphid's access to some essential nutrients, although there is no evidence that PP2s can bind nutrients present in phloem sap or in artificial diets for aphids, the composition of which is completely determined (holidic diet). Finally, this effect may result from the binding of PP2-A1-His$_6$ to glycoproteins in the midgut cells of the insects, or other internal targets, interfering with digestion, as observed for other plant lectins, potentially resulting in a postingestion antinutritional effect.

PP2-A1-His$_6$ had more moderate effects on *M. persicae* than on *A. pisum*, although each species reacted to the same range of protein concentrations. This suggests that adapted aphids are less susceptible to the effect of the lectin. Our results also confirmed the absence of an effect of the GlcNAc WGA lectin on aphid weight and survival (Fig. 8C), as reported previously (Rahbé and Febvay, 1993). The observation that PP2-A1-His$_6$, although not toxic for aphids, altered weight gain suggests a mechanism different from those reported for GlcNAc lectins, such as WGA, which are harmless to aphids. It may instead result from its $Man_3GlcNAc_2$ lectin activity, such moieties being abundant in insect glycoproteins. No significant effect was observed on weight gain for concentrations exceeding 500 μg mL^{-1} for the nymphs of both *A. pisum* and *M. persicae*. This lack of effect may result from aggregation of the recombinant protein in the artificial diet at such concentrations, making the protein less available for absorption from the diet. Protein aggregation has been observed in vitro at a concentration of 1,000 μg mL^{-1} in various buffers (D. Renard, unpublished data). The observation that, at a recombinant protein concentration of 500 μg mL^{-1}, *A. pisum* rejected the medium supplemented with PP2-

A1-His_6 in a choice test also suggests that, at high concentrations, this protein renders the medium unattractive to feeding aphids. Protein solutions are unlikely to affect the gustatory perception of the diet by aphids (Sauvion et al., 2004), so the simplest explanation would be that PP2-A1-His_6 alters the viscodynamic properties of the diet.

Further investigations to elucidate the role of PP2-A1 on aphid growth would benefit from the use of transgenic plants overexpressing the *PP2-A1* gene or *pp2-a1* knockout mutants. One *pp2-a1* insertion line has been described (Divol et al., 2007). Unfortunately, the level of expression of the *PP2-A1* gene was not affected by the insertion, which was located upstream from the promoter region; consistent with this finding, no effect on aphid settlement was observed (Divol et al., 2007), making it impossible to draw any firm conclusions about the role of PP2-A1 in vivo.

Survey of Phloem Sap Proteins

We checked the quality of the phloem sap isolated by EDTA-facilitated exudation by carrying out a survey of high-abundance phloem sap proteins based on LC-MS/MS. From the 27- and 55-kD fractions, we were able to characterize 24 proteins unambiguously (Supplemental Table S3). The relatively high frequency of glutathione *S*-transferase, dehydroascorbate reductase, catalase, copper ion-binding oxidoreductase, and enolase was consistent with the identification of oxidation-related or redox-related proteins in other reports of phloem sap protein analysis in other species (Walz et al., 2004; Giavalisco et al., 2006; Kehr, 2006). Three of the 24 proteins identified matched with orthologs found in the sap of *B. napus*: the UDP-Glc pyrophosphorylase UGP2, the glutathione *S*-transferase GSTF9, and the adenosylhomocysteinase SAHH1/HOG1 (Giavalisco et al., 2006). Several putative LRR-related proteins were also found. Two LRR proteins were found in *C. maxima* phloem sap (Lin et al., 2009). LRR domains are present in proteins with diverse functions, providing a framework for the formation of protein-protein interactions. In plants, they have been implicated in innate immunity signaling pathways (DeYoung and Innes, 2006). Several aphid resistance genes, conferring phloem-specific resistance, such as the *mi* gene in tomato (*Solanum lycopersicum*) and the *vat* gene in *C. melo*, encode nucleotide-binding site-LRR proteins (Kaloshian et al., 2000; Dogimont et al., 2008), suggesting a potential role, in sieve elements, in interactions with phloem-feeding insects.

PP2-A1 was not detected in the 27- and 55-kD fractions, although its theoretical molecular mass would be consistent with detection in these fractions. A PP2 lectin was previously detected in *B. napus* phloem sap, with an observed molecular mass smaller than expected (Giavalisco et al., 2006). The absence of PP2-A1 in these fractions may have resulted from a mobility shift on SDS-PAGE due to posttranslational modifications. Alternatively, PP2-A1 may not be mobile in sieve elements, instead remaining bound to structural elements (Oparka and Cruz, 2000). Indeed, in *C. maxima*, it has been suggested that the phloem lectin attaches the P-proteins to the sieve element reticulum or plasma membrane (Smith et al., 1987), although there is also evidence to suggest that a fraction is translocated over long distances through graft unions (Golecki et al., 1998, 1999). We also cannot rule out the possibility that the method used to collect phloem sap, involving the use of EDTA, a chelator of Ca^{2+} ions, affects the aggregation and mobility of PP2 proteins. Previous studies identifying PP2 phloem lectins in phloem sap proteomes were based on the collection of sap by phloem bleeding rather than EDTA-facilitated exudation (Walz et al., 2002, 2004; Giavalisco et al., 2006; Lin et al., 2009). Therefore, it remains unclear whether PP2-A1 subunits or small oligomers are mobile in the sieve elements of Arabidopsis or whether they are attached to sieve element membranes or to P-proteins. The extent to which PP2 aggregates may depend on the cellular environment and may be modified following the entry of the protein into the sieve elements. Based on our findings that this protein has two classes of sugar-binding sites, it will be interesting to investigate the subcellular distribution of this protein in vivo and to study the aggregation of PP2-A1 in different cell compartments or environmental conditions.

MATERIALS AND METHODS

Cloning of PP2-A1-His_6

Arabidopsis (*Arabidopsis thaliana* ecotype Columbia) was used for the cloning of the PP2-A1 cDNA. Total RNA was isolated from frozen tissues as described previously (Verwoerd et al., 1989). For initial cloning of the PP2-A1 cDNA, the coding sequence of the PP2-A1 cDNA previously amplified by RT-PCR from total RNA (forward primer A1-Fw, 5′-AAAAAAGCAGGCTCATGAGCAAGAAACATTGCTCAG-3′; reverse primer A1-Rv, 5′-AAGAAAGCTGGGTACTGTTTGGGACGAATTGCAAC-3′) was reamplified by PCR, with forward primer A1*Nde*I (5′-GGAATTCCATATGAGCAAGAAACATTGCTCA-3′) and reverse primer A1*Not*I (5′-TAAAGCGGCCGCAAATCAGTGGTGGTGGTGGTGCTGTTTGGGACGAATTGCAAC-3′). These primers were ordered from Biomers. They introduced an *Nde*I site at the 5′ end of the PCR product and a *Not*I restriction site at the 3′ end of the PCR product for further cloning (underlined sequences). PCR was performed in a GeneAmp 2700 PCR system from Applied Biosystems with *Taq* DNA polymerase (New England Biolabs). The following PCR conditions were used: 3 min of denaturation at 94°C, 25 cycles of 45 s at 94°C, 30 s at 55°C, and 1 min at 72°C, ending with an additional 7-min period of elongation at 72°C. The PCR product was purified with the QIAquick Gel Extraction kit (Qiagen) and inserted, as a *Nde*I/*Not*I fragment, into a modified pET9 vector (Novagen) into which a new *Not*I site had been introduced, to create the expression plasmid pET9-PP2-A1, for the expression of a translational fusion of PP2-A1 with a C-terminal six-His tag under the control of the T7 promoter. For the shorter sequence of PP2-A1, forward primer A1Fw (5′-TTTAGAAACCAAGACTCGAAA-3′) and reverse primer A1bis*Not*I (5′-TAAAGCGGCCGCAAATCAGTG-3′) were used to amplify the sequence from the pET9-PP2-A1 clone, which already contains the His tag sequence. The A1bis*Nde*I primer (5′-GGAATTCCATATGTTTAGAAACCAAGACTCGAAA-3′) was used with the A1bis*Not*1 primer to introduce restriction sites for subsequent insertion into the pET9 vector, yielding pET9-PP2-A1s. PCR was performed as described above, with the following modifications: 30 cycles, with annealing at 54°C.

The plasmids were transferred into *Escherichia coli* DH5α, in a transformation procedure involving the incubation of 150 ng of plasmid DNA with

thermocompetent cells (Invitrogen) for 45 s at 42°C, followed by the addition of 2YT medium (4 g L^{-1} bactotryptone, 2.5 g L^{-1} yeast extract, and 1.25 g L^{-1} NaCl) and incubation for 1 h at 37°C. The cells were then resuspended in 2YT supplemented with kanamycin (50 μg mL^{-1}) and incubated overnight at 37°C. The inserts present in the pET9-PP2-A1 and pET9-PP2-A1s plasmids were confirmed by sequencing (Millegen Service Facility) using 5′T7 promoter and terminator primers.

Large-Scale Production of PP2-A1-His_6

For large-scale protein production, the plasmids were introduced into *E. coli* Tuner DE3 pLysS cells (Novagen). We used 10 mL of a fresh culture in 2YT medium supplemented with kanamycin (50 μg mL^{-1}) and chloramphenicol (34 μg mL^{-1}) incubated overnight at 37°C to inoculate 4 L of 2YT medium in a fermentor (Applicon) equipped for the maintenance of constant aeration levels, pH (7), and temperature (37°C). Production of the recombinant protein was induced by adding 1 mM isopropyl β-D-thiogalactopyranoside to the culture when it reached an optical density at 600 nm of 1.5. After 3 h of induction, the cells were harvested by centrifugation (20 min, 5,000*g*) at 4°C. The pellet was frozen at –20°C. For purification purposes, we typically dissolved 5 mg of pellet (one-fifth of the total pellet) in 30 mL of extraction buffer (50 mM Tris, 200 mM NaCl, and 10 mM imidazole, pH 8). Two freeze-thaw cycles were carried out at −20°C/+20°C and −176°C (liquid nitrogen)/+20°C, and the samples were sonicated for 90 s, with 10-s pulses of 80 W, at 4°C. The lysate was centrifuged for 45 min at 12,000*g* and room temperature. The supernatant was then loaded onto a 30-mL fast-flow nickel affinity column (GE, Amersham) equilibrated with extraction buffer (50 mM Tris, 200 mM NaCl, and 10 mM imidazole, pH 8). Proteins were eluted from the column (AKTA-PRIME; GE, Amersham) in an imidazole gradient of 250 to 500 mM in extraction buffer. Ten 5-mL fractions, corresponding to the protein elution profile, were typically collected after purification.

Fractions were dialyzed (Spectra/Por Membrane; molecular weight cutoff, 6–8,000) four times against 500 volumes of water to remove salts and imidazole. The various fractions were then immediately frozen at −20°C and freeze-dried. Lyophilized PP2-A1-His_6 protein was stored in a desiccator in the dark. Proteins were analyzed by SDS-PAGE (Laemmli, 1970) on 12% or 15% Tris-HCl polyacrylamide gels. Before electrophoresis, the samples were boiled for 2 min in 2× Laemmli sample buffer. After electrophoresis, the proteins were detected by staining the gels for 30 min at room temperature with Coomassie Brilliant Blue R (Bio-Rad).

Characterization of the Recombinant Protein by MS

MS analyses were conducted at the Biopolymers-Interactions-Structural Biology platform of the INRA Center at Nantes (http://www.nantes.inra.fr/plateformes_et_plateaux_techniques/plateforme_bibs). The molecular mass of purified PP2-A1-His_6 was determined with an ion-trap mass spectrometer (LCQ Advantage; Thermo-Fisher) equipped with an ESI source operating in the positive ion mode. Samples were solubilized at a concentration of 20 nmol mL^{-1} in an aqueous mixture of water and acetonitrile (1:1, v/v) acidified with 0.1% formic acid. Samples were infused into the mass spectrometer at a continuous flow rate of 5 μL min^{-1}. Mass data were acquired for the mass-to-charge (*m/z*) range 400 to 2,000.

The sequence of PP2-A1-His_6 was determined, after trypsin hydrolysis of the protein, by MALDI mass measurement for the resulting peptides. We solubilized 50 μg of purified PP2-A1-His_6 in a 25 mM ammonium bicarbonate buffer (pH 8.5) and subjected the resulting solution to trypsin treatment (Promega) for 3 h at 37°C (enzyme:substrate ratio 1:30 [w/w]). The resulting mixture of peptides was diluted 1:50 in water. We mixed 1 μL of the dilution with 1 μL of the matrix preparation (2.5 mg mL^{-1} cyano-4-hydroxycinnamic acid, 2.5 mg mL^{-1} 2,5-dihydroxybenzoic acid, 70% [v/v] acetonitrile, and 0.1% [v/v] trifluoroacetic acid) and deposited the mixture on the MALDI sample probe. MALDI-time-of-flight-MS was performed for the 850 to 3,500 *m/z* range on a M@LDI LR instrument (Waters) equipped with a conventional nitrogen laser (337 nm) operating at a frequency of 10 Hz.

The smallest peptides generated by trypsin digestion were further analyzed by MS/MS fragmentation, based on nanoflow ESI-MS/MS on a hybrid quadrupole orthogonal acceleration time-of-flight mass spectrometer (Q-TOF Global; Waters). The products of the trypsin digestion were diluted 1:100 in an aqueous mixture of water and acetonitrile (1:1, v/v) acidified with 0.1% formic acid. We introduced 2 μL of the resulting mixture into a metal-coated glass capillary (Proxeon) and allowed it to infuse into the mass spectrometer at an approximate flow rate of 100 nL min^{-1}. Mass data were acquired for the 300 to 2,000 *m/z* range. The peptide at M_{H+} 1.0404 kD (doubly charged ion at *m/z* 520.7) was fragmented by collision-induced dissociation, and fragments were measured over the 20 to 1,200 *m/z* range. The fragment ions were compared with the theoretical b and y ions generated by the 5 to 13 sequence of PP2-A1-His_6 (HCSELLPNK) using Mass Lynx Biotools software (Waters).

Chitin Column Binding Assay

For this assay, we used the bacterial strains harboring the longer PP1-A1-His_6 initially generated. The pellet recovered from 5 mL of culture, resulting in production of the recombinant PP2-A1-His_6 protein, was solubilized in extraction buffer (50 mM Tris and 200 mM NaCl, pH 8) and cells were sonicated (1.5 min, 10-s pulse, 80 kHz, 4°C). The bacterial extract was applied to a 5-mL GlcNAc-Sepharose column (New England Biolabs). Unbound proteins were removed by washing the column twice with 5 mL of extraction buffer. Finally, successive washes with 5 mL of NaOH solutions at concentrations of 0.05, 0.1, and 0.5 M resulted in desorption of the bound PP2-A1-His_6. The eluted proteins were analyzed by SDS-PAGE on a 15% polyacrylamide gel, as described above, with detection by Coomassie Brilliant Blue staining.

Glycan Array Binding Affinity of PP2-A1-His_6

PP2-A1-His_6 was used to probe the printed glycan microarrays according to the standard procedure of Core H of the Consortium for Functional Glycomics (https://www.functionalglycomics.org/static/consortium/resources/resourcecoreh8.shtml), version 3.1, being used for the analyses reported here. This printed array consists of 377 glycans in replicates of six. Lyophilized recombinant protein was dissolved in Tris-buffered saline (20 mM Tris-HCl, 150 mM NaCl, 2 mM $CaCl_2$, and 2 mM $MgCl_2$, pH 7.4, containing 0.05% Tween 20 and 1% bovine serum albumin) to a concentration of 1 mg mL^{-1}, and this solution was diluted to give a final concentration of 0.1, 10, 50, or 100 μg mL^{-1}. Aliquots (70 μL) of PP2-A1-His_6 at the appropriate concentration were applied to each well of the printed microarray. The binding of PP2-A1-His_6 to specific glycans was detected and quantified as described previously (Subramanyam et al., 2008), except that recombinant PP2-A1-His_6 was detected with a commercial antibody against the His_6 tag. Binding was quantified by fluorescence techniques, and the data are expressed as mean numbers of relative fluorescence units for the replicates for each glycan represented on the array.

Surface Plasmon Resonance

Surface plasmon resonance analyses (Achilleos et al., 2009) were performed on a BIAcore 3000 optical biosensor equipped with a research-grade carboxymethyl dextran CM5 sensor chip (GE Healthcare). For PP2-A1-His_6 immobilization, the carboxyl groups of the CM5 sensorchip were activated at a flow rate of 20 μL min^{-1} with a 10-min pulse of *N*-hydroxysuccinimide and 1-ethyl-3-(3-dimethylaminopropyl) carbodiimide hydrochloride (1:1 mixture). We then injected 100 μg mL^{-1} PP2-A1 in 10 mM acetate buffer, pH 5, for approximately 10 min and blocked the remaining succinimidyl esters by injecting 1 M ethanolamine hydrochloride, pH 8.5, for 10 min. The immobilization of about 2,000 RU was achieved with the Biacore 3000 in these immobilization conditions. For binding experiments, the *N*,*N*′,*N*″-triacetylchitotriose solution (Sigma) was diluted in 10 mM HEPES, 3 mM EDTA, 0.15 M sodium chloride, 0.005% P_2O, pH 7.4, running buffer at various concentrations (0, 5, 10, 20, 50, 100, 150, 200, 400, 600, 800, and 1,000 μg mL^{-1}). The resulting solutions were passed over the PP2-A1-His_6 immobilized on the CM5 surface at a flow rate of 20 μL min^{-1} and a temperature of 25°C. Surface regeneration was achieved by injecting 50 mM NaOH into the system. PP2-A1-His_6 solution was injected over two channels at a flow rate of 20 μL min^{-1}. In one of these channels, the CM5 surface was activated with *N*-hydroxysuccinimide:1-ethyl-3-(3-dimethylaminopropyl) carbodiimide hydrochloride (channel response), whereas in the other channel, the surface was not activated (reference channel response). The specific response (or response difference) was obtained by subtracting the reference channel response from the channel response. R_{max} was defined as $R_{max} = (M_{r\ N,N',N''\text{-triacetylchitotriose}}/M_{r\ \text{PP2-A1-His6}}) \times \text{RU}$ immobilized $\times$ *S*, where *S* is the stoichiometry. With *N*,*N*′,*N*″-triacetylchitotriose (M_r = 627) and PP2-A1-His_6 (M_r approximately 28,000), R_{max} is predicted to be close to 45 RU for a stoichiometry of 1:1 [(627/28,000) × 2,000 × 1 = 44.8 RU].

Fluorescence Spectroscopy

Titrations of PP2-A1-His_6 with *N*,*N*′,*N*″-triacetylchitotriose (Sigma) were performed by intrinsic fluorescence spectroscopy. We added 0.7-μg aliquots of *N*,*N*′,*N*″-triacetylchitotriose (0.138 mg mL^{-1}) stepwise to the protein solution (0.175 mg mL^{-1}) to obtain a protein-to-sugar molar ratio of 0 to 10. PP2-A1-His_6 was dissolved in "universal" buffer solution (Britton and Robinson type) at pH 8. Universal buffer contained citric acid, KH_2PO_4, H_3BO_4, and diethylbarbituric acid, and its pH was adjusted by titrating the solution with 0.2 M NaOH (Johnson and Lindsey, 1939; Britton, 1955). Intrinsic fluorescence spectra were recorded on a Fluoromax-Spex (Jobin-Yvon) at 25°C using an excitation wavelength of 290 nm. Spectra were collected with a step resolution of 1 nm and emission and excitation slits fixed at 5 nm. All spectra were corrected for the solvent (buffer in the presence of *N*,*N*′,*N*″-triacetylchitotriose) in the 300- to 450-nm regions using a 1-cm path length. Spectra were recorded in duplicate. The fluorescence intensity corresponding to sugar/protein complex formation during titration was used to calculate the binding parameters K_d and n by the fitting of a Scatchard regression line (Scatchard, 1949).

In this case, the Scatchard equation was applied assuming a noncooperative model with independent and nonidentical sites. The equation used in this case is: $S_b/S_f = -S_b/K_d + nP_t/K_d$, where S_b is the bound sugar concentration (M), S_f the free sugar concentration (M), and P_t the total protein concentration (M). The S_b/P_t ratio was given by the $F - F_0/F_{max} - F_0$ data values corresponding to the fluorescence of the sugar/protein complex. The free sugar concentration S_f was deduced from S_b/P_t values and total sugar concentration. The Scatchard representation displays $S_b/S_f \times P_t$ as a function of S_b/P_t.

Sequence Analysis

Searches for motifs and sites of posttranslational modifications, such as glycosylation and phosphorylation, were carried out with Prosite (http://expasy.org/prosite; Sigrist et al., 2002). Multiple alignments were established with Multalin (http://bioinfo.genopole-toulouse.prd.fr/multalin/multalin.html). We searched for lectin domains with Prosite and Pfam (http://pfam.sanger.ac.uk/).

Phloem Sap Exudation

Phloem sap was obtained by EDTA-facilitated exudation (King and Zeevaart, 1974). Four- to 6-week-old plants were grown in a greenhouse (16-h photoperiod). Mature rosette leaves were cut at the base of the petiole and a second cut was made next to the first cut, in exudation buffer (50 mM potassium phosphate buffer, pH 7.6, 10 mM EDTA). The tip of the petiole was placed in 80 μL of exudation buffer in a 2-mL Eppendorf tube. Standard exudation experiments were carried out for 6 h, in the dark, in a closed box containing wet paper to limit transpiration and to maintain humidity in growth cabinets (20°C, 75% relative humidity). Samples were pooled and concentrated on centrifugal filter devices with a cutoff of 10 kD (Centricon; Millipore). The sugars in the phloem sap exudates were analyzed in an enzymatic assay based on a commercial kit for determining Suc and hexoses (Suc/D-Glc/D-Fru kit RBIOPHARM).

Analysis of Phloem Sap Proteins by Enzymatic Glucosidase Treatments

For PNGaseF enzymatic treatment, the content of exudate samples was adjusted such that the exudate was essentially in PNGaseF reaction buffer (50 mM phosphate buffer, pH 7.5, 0.1% SDS, and 50 mM β-mercaptoethanol) and the samples were then boiled for 5 min. We added 0.7% Triton X-100 and 5 units of PNGase F (Sigma) and incubated the mixture overnight at 37°C. For GDase enzymatic treatment, the content of the exudate samples was adjusted to the GDase reaction buffer (50 mM citrate buffer, pH 5, 100 mM NaCl, and 0.01% bovine serum albumin). We then added 5 mM *N*-acetyl β-D-glucosaminide and 0.01 unit of GDase (Sigma). The mixture was incubated overnight at 25°C. Proteins were analyzed by SDS-PAGE on a 12% polyacrylamide gel. Proteins were visualized by staining with SYPRO Ruby (Bio-Rad) for visualization at 580 nm with a phosphoimager or blotted onto nitrocellulose or polyvinylidene fluoride membranes (Bio-Rad) for far-western immunodetection.

Far-Western Blots

For protein overlay experiments (far-western blots), the membranes onto which the proteins had been transferred were blocked by incubation for 1 h with 5% nonfat milk powder in phosphate-buffered saline (PBS) supplemented with 0.1% Tween 20 (PBS-T). They were then incubated for 1 h at room temperature with the recombinant PP2A1-His_6 (10 μg mL^{-1}) in PBS-T. The recombinant protein was detected by incubation for 1 h at room temperature in PBS-T with a commercial peroxidase-conjugated mouse monoclonal antibody against His (Roche; 50 milliunits mL^{-1}; 1/1,000) for the detection of His-tagged recombinant proteins. Peroxidase activity was detected with the Immun-Star horseradish peroxidase chemiluminescence kit (Bio-Rad). The experiments were repeated five times.

Analysis of Phloem Sap Proteins by LC-MS/MS

Phloem sap proteins were separated by SDS-PAGE on 12% polyacrylamide gels. The gel was stained with Sypro Ruby (Bio-Rad), and the two main bands were excised (2 mm in width) and analyzed by the PAPPSO platform (http://moulon.inra.fr/PAPPSO/analyses.html). The proteins were subjected to in-gel digestion with the Progest system (Genomic Solution) as follows. Gel pieces were washed in successive baths of (1) 10% acetic acid and 40% ethanol and (2) 100% acetonitrile. They were then washed in successive baths of (1) 25 mM NH_4CO_3 and (2) 100% acetonitrile. A volume of 40 μL was used for each bath. Gel pieces were then incubated in 40 μL of 10 mM dithiothreitol in 25 mM NH_4CO_3, for 30 min at 55°C, and in 30 μL of 50 mM iodoacetamide in 25 mM NH_4CO_3, for 45 min at room temperature, for Cys reduction and alkylation, respectively. Proteins were subsequently digested for 6 h at 37°C with 20 μL of 125 ng of modified trypsin (Promega) dissolved in 20% methanol and 20 mM NH_4CO_3 per gel piece. The peptides were extracted successively with (1) 20 μL of 0.5% trifluoroacetic acid and 50% acetonitrile and (2) 20 μL of 100% acetonitrile. The resulting peptide extracts were dried in a vacuum centrifuge and suspended in 25 μL of 0.08% trifluoroacetic acid and 2% acetonitrile for LC-MS/MS analysis. LC-MS/MS was performed on an Ultimate 3000 LC system (Dionex) connected to an LTQ Orbitrap mass spectrometer (Thermo Fisher) with a nanoelectrospray ion source. Tryptic peptide mixtures were loaded onto the Pepmap C18 (0.3 × 5 mm, 100 Å, 5 μm; Dionex) at a flow rate of 20 μL min^{-1}. After 4 min, the precolumn was connected to the Pepmap C18 (0.075 × 15 cm, 100 Å, 3 μm) separating nanocolumn and a linear gradient was established, from 2% to 36% buffer B (0.1% formic acid and 80% acetonitrile) in buffer A (0.1% formic acid and 2% acetonitrile), at a flow rate of 300 nL min^{-1} over 50 min. Ionization was performed at the liquid junction, with a spray voltage of 1.3 kV applied to an uncoated capillary probe (PicoTip EMITER 10-μm tip ID; New Objective). Peptide ions were automatically analyzed by the data-dependent method, as follows: full MS scan (m/z 300–1,600) on an Orbitrap analyzer and MS/MS on the four most abundant precursors, with the LTQ linear ion trap. In this study, only +2 and +3 charged peptides were subjected to MS/MS, with an exclusion window of 1.5 min, using classical peptide fragmentation parameters: Qz = 0.22, activation time = 50 ms, collision energy = 35%.

The raw data generated by the LTQ-Orbitrap mass spectrometer were first converted into an mzXML file with ReADW (http://sashimi.sourceforge.net). Proteins were then identified with X!Tandem software 1 (X!Tandem tornado 2008.02.01.3; http://www.thegpm.org) used against an Arabidopsis protein database associated with a proteomic contaminant database. The X!Tandem search parameters were as follows: trypsin specificity with a tolerance of one missed cleavage, fixed alkylation of Cys, and variable oxidation of Met. The mass tolerance was fixed to 10 ppm for precursor ions and 0.5 D for fragment ions. The final search results were filtered with a multiple threshold filter applied at the protein level and consisted of the following criteria: protein identified with a minimum of nine different peptide sequences detected with a peptide *E*-value of less than 0.05.

Three-Dimensional Modeling of PP2-A1

We carried out protein analysis with PROSAL, which provides links to a full range of Web analyses for protein primary sequences (http://xray.bmc.uu.se/sbnet/prosal.html). Tertiary structure was predicted by searching for similarity to proteins with structures solved with the CBS@tome2 metaserver (http://abcis.cbs.cnrs.fr/AT2/meta.html). This analysis includes the TITO program (Labesse and Mornon, 1998), which can align sequences when the level of sequence identity between a query sequence and a three-dimensional

structure is low (10%–30%). The results were validated by searches with other metaservers, such as BioInfo Bank (http://meta.bioinfo.pl/3djury.pl), using the 3D-Jury method (Ginalski et al., 2003; von Grotthuss et al., 2003), Fold Recognition Server (version 2.6.0; http://www.sbg.bio.ic.ac.uk/servers/3dpssm/) with the 3D-PSSM program (Kelley et al., 2000), and the PHYRE Web server (http://www.sbg.bio.ic.ac.uk/phyre/html/index.html). A three-dimensional model was prepared with MacPyMOL software. The accession numbers for CBMs are as follows. For the Cbm4 of the laminarase 16a (lam16a) from the bacterium *Thermotoga maritima*: PDB, 1gui1; GenBank, Q9WXN1; for the Cbm22-2 of the endo-1,4-β-xylanase Y (Xyn10B) from *Clostridium thermocellum*: PDB, 1H6Y.

Aphid Artificial Diet Bioassay

The stock population of *Acyrthosiphon pisum* (clone LL01) was maintained in the laboratory on broad bean (*Vicia faba*), as previously described (Febvay et al., 1988). The stock population of *Myzus persicae* ("green" LC05 clone originating from INRA Colmar, and "pink" L06 clone collected on pepper in Lyon) was maintained on pepper (*Capsicum annuum*). For both aphid species, the experiments were conducted on neonate aphid nymphs reared on aphid diet formulation AP3 (Febvay et al., 1988). In addition to microelements and macroelements, this diet contains 584 mM Suc and 260 mmol L^{-1} amino acids. These conditions are typical of the sugar and nitrogen content of phloem sap. The medium was supplemented with various concentrations, from 0 to 1,000 μg mL^{-1}, of recombinant PP2-A1-His_6 (at concentrations of 0.01, 16, 32, 64, 125, 250, 500, or 1,000 μg mL^{-1} for biological replicate 1 and 0.01, 32, 125, or 500 μg mL^{-1} for biological replicate 2 with *A. pisum*; at concentrations of 28, 83, 250, or 750 μg mL^{-1} for experiments with *M. persicae* L06 and LC05 clones for biological replicate 1 and 0.01, 50, 100, 200, 300, and 500 μg mL^{-1} for biological replicate 2), casein (Sigma) used as a negative control, or WGA (Sigma L9640) used as a control GlcNAc lectin (at a concentration of 28, 83, 250, or 750 μg mL^{-1}). These concentrations are typical of those generally used in lectin bioassays in aphids (Rahbé and Febvay, 1993). Ampicillin (50 μg mL^{-1}), an antibiotic harmless to the aphid primary symbiont *Buchnera*, was added to the medium to prevent microbial contamination. For each concentration of recombinant protein, we transferred 25 to 40 neonate nymphs directly onto artificial diet medium, on which they were maintained at 20°C for 7 d. For the control proteins, casein and WGA, 18 neonate nymphs were used per concentration. The biological performance of PP2-A1-His_6 was estimated by assessing mortality during development and by weighing aphids after the adult molt (measured on a 1-μg sensitive Setaram balance for *M. persicae* and a 10-μg sensitive balance for *A. pisum*). All experiments were carried out at 20°C, 75% relative humidity, and a photoperiod of 16 h of light/8 h of darkness. The results were statistically analyzed, using ANOVA and common posthoc tests, including Dunnet's tests (JMP Software version 8; SAS Institute). In these experiments, aphid behavior was evaluated by scoring aphid settlement, measured after 24 h by counting the number of aphids successfully feeding on the artificial medium.

The choice test was carried out as described (Chen et al., 1996). Briefly, six neonate aphids were deposited in cylindrical boxes containing two diet tubes (one containing aphid diet medium and one containing aphid diet medium supplemented with PP2-A1-His_6), which were left overnight in a dark box for 16 h, before scoring for each set of conditions. The experiment was repeated at least 18 times for each choice situation. Two concentrations of PP2-A1-His_6 were tested: 200 and 500 μg mL^{-1}. For each set of conditions, the phagostimulation index (Ix) was calculated as follows: $Ix = T - C/T + C$, where T = number of aphids on medium supplemented with PP2-A1-His_6 (test) and C = number of aphids on control medium. The results were analyzed with a nonparametric paired-data method (Wilcoxon's signed rank test; JMP Software).

The accession numbers for the PP2s analyzed in this work are as follows: AtPP2-A1, O81865; CbmLec26, CAA78979; CbpLec26, CAA80364; CsLec26, AAM82557; CsLec17, AAM77344; CmmLec17, AAM77341; CmmLec26, AAM74921; AgPP2-1, AAM62132; Nictaba, AAK84134. The nucleotide sequence accession number for *PP2-A1* is At4g19840.

Supplemental Data

The following materials are available in the online version of this article.

Supplemental Figure S1. Peptide coverage of PP2-A1-His_6 by MS.

Supplemental Figure S2. Effect of PP2-A1-His_6 on the growth of two clones of *M. persicae*.

Supplemental Table S1. Glycan array data.

Supplemental Table S2. Phloem sap proteins identified by LC-MS/MS.

Supplemental Table S3. Feeding bioassay with artificial diet on *A. pisum* and *M. persicae*.

Supplemental Table S4. Choice tests on *A. pisum* and *M. persicae*.

ACKNOWLEDGMENTS

We thank H. Rogniaux and A. Geairon (INRA, UR1268, BIBS Platform, Nantes, France) for the MS analyses, G. Duport and M. Pichon (INSA-INRA, Lyon, France) for the diet experiments on aphids, J.P. Compoint (INRA, UR1268, Nantes, France) for fruitful discussions on the PP2-A1 purification procedure, and Dr. M. Gonneau (LCB, Versailles, France) and Dr. A. Guillot (INRA, UR477, PAPPSO Platform, Jouy en Josas, France) for LC-MS/MS analyses. We thank T. Lemaître (INRA, IJPB, Versailles, France) for discussions and the Consortium for Functional Glycomics and Dr. D. Smith (Emory University School of Medicine, Atlanta) for providing the resources and carrying out the glycan microarray analyses. We thank S. Bouhallab (INRA, UMR 1253, Rennes, France) for help with fluorescence data processing and Dr. G. Labesse (CNRS, Centre de Biochimie Structurale, Montpellier, France) for help with PP2-A1 three-dimensional structure prediction. We thank OUEST-GENOPOLE for contributing to the recombinant protein work.

Received January 26, 2010; accepted April 28, 2010; published May 4, 2010.

LITERATURE CITED

Achilleos C, Tailhardat M, Courtellemont P, Varlet BL, Dupont D (2009) Investigation of surface plasmon resonance biosensor for skin sensitizers studies. Toxicol In Vitro **23:** 308–318

Alexandrov NN, Troukhan ME, Brover VV, Tatarinova T, Flavell RB, Feldmann KA (2006) Features of Arabidopsis genes and genome discovered using full-length cDNAs. Plant Mol Biol **60:** 69–85

Allen AK (1979) A lectin from the exudate of the fruit of the vegetable marrow (*Cucurbita pepo*) that has a specificity for beta-1,4-linked N-acetylglucosamine oligosaccharides. Biochem J **183:** 133–137

Aoki K, Kragler F, Xoconostle-Cazares B, Lucas WJ (2002) A subclass of plant heat shock cognate 70 chaperones carries a motif that facilitates trafficking through plasmodesmata. Proc Natl Acad Sci USA **99:** 16342–16347

Aoki K, Suzui N, Fujimaki S, Dohmae N, Yonekura-Sakakibara K, Fujiwara T, Hayashi H, Yamaya T, Sakakibara H (2005) Destination-selective long-distance movement of phloem proteins. Plant Cell **17:** 1801–1814

Balachandran S, Xiang Y, Schobert C, Thompson GA, Lucas WJ (1997) Phloem sap proteins from *Cucurbita maxima* and *Ricinus communis* have the capacity to traffic cell to cell through plasmodesmata. Proc Natl Acad Sci USA **94:** 14150–14155

Banerjee S, Hess D, Majumder P, Roy D, Das S (2004) The interactions of *Allium sativum* leaf agglutinin with a chaperonin group of unique receptor protein isolated from a bacterial endosymbiont of the mustard aphid. J Biol Chem **279:** 23782–23789

Barnes A, Bale J, Constantinidou C, Ashton P, Jones A, Pritchard J (2004) Determining protein identity from sieve element sap in *Ricinus communis* L. by quadrupole time of flight (Q-TOF) mass spectrometry. J Exp Bot **55:** 1473–1481

Bencharki B, Boissinot S, Revollon S, Ziegler-Graff V, Erdinger M, Wiss L, Dinant S, Renard D, Beuve M, Lemaitre-Guillier CV, et al (2010) Phloem protein partners of Cucurbit aphid borne yellows virus: possible involvement of phloem proteins in virus transmission by aphids. Mol Plant Microbe Interact **23:** 799–810

Beyenbach J, Weber C, Kleinig H (1974) Sieve-tube proteins from *Cucurbita maxima*. Planta **119:** 113–124

Blixt O, Head S, Mondala T, Scanlan C, Huflejt ME, Alvarez R, Bryan MC, Fazio F, Calarese D, Stevens J, et al (2004) Printed covalent glycan array for ligand profiling of diverse glycan binding proteins. Proc Natl Acad Sci USA **101:** 17033–17038

Boraston AB, Nurizzo D, Notenboom V, Ducros V, Rose DR, Kilburn DG, Davies GJ (2002) Differential oligosaccharide recognition by evolution-

arily-related beta-1,4 and beta-1,3 glucan-binding modules. J Mol Biol **319:** 1143–1156

Bostwick DE, Dannenhoffer JM, Skaggs MI, Lister RM, Larkins BA, Thompson GA (1992) Pumpkin phloem lectin genes are specifically expressed in companion cells. Plant Cell **4:** 1539–1548

Bostwick DE, Skaggs MI, Thompson GA (1994) Organization and characterization of *Cucurbita* phloem lectin genes. Plant Mol Biol **26:** 887–897

Britton HTS (1955) Hydrogen Ions: Their Determination and Importance in Pure and Industrial Chemistry, Ed 4, Vol 3. Chapman & Hall, London

Carlini CR, Grossi-de-Sa MF (2002) Plant toxic proteins with insecticidal properties: a review on their potentialities as bioinsecticides. Toxicon **40:** 1515–1539

Chen D, Juarez S, Hartweck L, Alamillo JM, Simon-Mateo C, Perez JJ, Fernandez-Fernandez MR, Olszewski NE, Garcia JA (2005) Identification of secret agent as the O-GlcNAc transferase that participates in plum pox virus infection. J Virol **79:** 9381–9387

Chen JQ, Delobel B, Rahbé Y, Sauvion N (1996) Biological and chemical characteristics of a genetic resistance of melon to the melon aphid. Entomol Exp Appl **80:** 250–253

Chen Y, Peumans WJ, Hause B, Bras J, Kumar M, Proost P, Barre A, Rouge P, Van Damme EJ (2002) Jasmonic acid methyl ester induces the synthesis of a cytoplasmic/nuclear chito-oligosaccharide binding lectin in tobacco leaves. FASEB J **16:** 905–907

Clark AM, Jacobsen KR, Bostwick DE, Dannenhoffer JM, Skaggs MI, Thompson GA (1997) Molecular characterization of a phloem-specific gene encoding the filament protein, phloem protein 1 (PP1), from *Cucurbita maxima*. Plant J **12:** 49–61

Corbesier L, Vincent C, Jang S, Fornara F, Fan Q, Searle I, Giakountis A, Farrona S, Gissot L, Turnbull C, et al (2007) FT protein movement contributes to long-distance signaling in floral induction of Arabidopsis. Science **316:** 1030–1033

Dannenhoffer JM, Schulz A, Skaggs MI, Bostwick DE, Thompson GA (1997) Expression of the phloem lectin is developmentally linked to vascular differentiation in cucurbits. Planta **201:** 405–414

de Jesus Perez J, Juarez S, Chen D, Scott CL, Hartweck LM, Olszewski NE, Garcia JA (2006) Mapping of two O-GlcNAc modification sites in the capsid protein of the potyvirus Plum pox virus. FEBS Lett **580:** 5822–5828

DeYoung BJ, Innes RW (2006) Plant NBS-LRR proteins in pathogen sensing and host defense. Nat Immunol **7:** 1243–1249

Dinant S, Bonnemain J, Girousse C, Kehr J (2010) Phloem sap intricacy and interplay with aphid feeding. C R Biol **333:** 504–515

Dinant S, Clark AM, Zhu Y, Vilaine F, Palauqui JC, Kusiak C, Thompson GA (2003) Diversity of the superfamily of phloem lectins (phloem protein 2) in angiosperms. Plant Physiol **131:** 114–128

Dinant S, Lemoine R (2010) The phloem pathway: new issues and old debates. C R Biol **333:** 307–319

Divol F, Vilaine F, Thibivilliers S, Kusiak C, Sauge MH, Dinant S (2007) Involvement of the xyloglucan endotransglycosylase/hydrolases encoded by celery XTH1 and Arabidopsis XTH33 in the phloem response to aphids. Plant Cell Environ **30:** 187–201

Dogimont C, Chovelon V, Tual S, Boissot N, Rittener V, Giovinazzo N, Bendahmane A (2008) Molecular diversity at the *Vat/Pm-W* resistance locus in melon. *In* M Pitrat, ed, IXth EUCARPIA Meeting on Genetics and Breeding of Cucurbitaceae. INRA, Avignon, France, pp 219–227

Esau K, editor (1969) The Phloem: Encyclopedia of Plant Anatomy, Vol 5. Gebrüder Borntraegger, Berlin-Stuttgart

Evert R (1990) Dicotyledons. *In* H-D Behnke, R Sjölund, eds, Sieve Elements. Comparative Structure, Induction and Development. Springer-Verlag, Berlin, pp 103–137

Febvay G, Delobel B, Rahbé Y (1988) Influence of the amino acid balance on the improvement of an artificial diet for a biotype of *Acyrthosiphon pisum* (Homoptera: Aphididae). Can J Zool **66:** 2449–2453

Giavalisco P, Kapitza K, Kolasa A, Buhtz A, Kehr J (2006) Towards the proteome of *Brassica napus* phloem sap. Proteomics **6:** 896–909

Ginalski K, Elofsson A, Fischer D, Rychlewski L (2003) 3D-Jury: a simple approach to improve protein structure predictions. Bioinformatics **19:** 1015–1018

Golecki B, Schulz A, Carstens-Behrens U, Kollmann R (1998) Evidence for graft transmission of structural phloem proteins or their precursors in heterografts of Cucurbitaceae. Planta **206:** 630–640

Golecki B, Schulz A, Thompson GA (1999) Translocation of structural P proteins in the phloem. Plant Cell **11:** 127–140

Gómez G, Pallás V (2001) Identification of an *in vitro* ribonucleoprotein complex between a viroid RNA and a phloem protein from cucumber plants. Mol Plant Microbe Interact **14:** 910–913

Gómez G, Pallás V (2004) A long-distance translocatable phloem protein from cucumber forms a ribonucleoprotein complex *in vivo* with hop stunt viroid RNA. J Virol **78:** 10104–10110

Gómez G, Torres H, Pallás V (2005) Identification of translocatable RNA-binding phloem proteins from melon, potential components of the long-distance RNA transport system. Plant J **41:** 107–116

Ham BK, Brandom JL, Xoconostle-Cazares B, Ringgold V, Lough TJ, Lucas WJ (2009) A polypyrimidine tract binding protein, pumpkin RBP50, forms the basis of a phloem-mobile ribonucleoprotein complex. Plant Cell **21:** 197–215

Hanover JA (2001) Glycan-dependent signaling: O-linked N-acetylglucosamine. FASEB J **15:** 1865–1876

Hart GW, Housley MP, Slawson C (2007) Cycling of O-linked beta-N-acetylglucosamine on nucleocytoplasmic proteins. Nature **446:** 1017–1022

Hayashi H, Fukuda A, Suzui N, Fujimaki S (2000) Proteins in the sieve element-companion cell complexes: their detection, localization and possible functions. Aust J Plant Physiol **27:** 489–496

Heese-Peck A, Cole RN, Borkhsenious ON, Hart GW, Raikhel NV (1995) Plant nuclear pore complex proteins are modified by novel oligosaccharides with terminal N-acetylglucosamine. Plant Cell **7:** 1459–1471

Hollister J, Grabenhorst E, Nimtz M, Conradt H, Jarvis DL (2002) Engineering the protein N-glycosylation pathway in insect cells for production of biantennary, complex N-glycans. Biochemistry **41:** 15093–15104

Ivashikina N, Deeken R, Ache P, Kranz E, Pommerrenig B, Sauer N, Hedrich R (2003) Isolation of *AtSUC2* promoter-*GFP*-marked companion cells for patch-clamp studies and expression profiling. Plant J **36:** 931–945

Johnson WC, Lindsey AJ (1939) An improved universal buffer. Analyst (Lond) **64:** 490–492

Kaloshian I, Kinsey MG, Williamson VM, Ullman DE (2000) Mi-mediated resistance against the potato aphid *Macrosiphum euphorbiae* (Hemiptera: Aphididae) limits sieve element ingestion. Environ Entomol **29:** 690–695

Kehr J (2006) Phloem sap proteins: their identities and potential roles in the interaction between plants and phloem-feeding insects. J Exp Bot **57:** 767–774

Kehr J, Buhtz A (2008) Long distance transport and movement of RNA through the phloem. J Exp Bot **59:** 85–92

Kelley LA, MacCallum RM, Sternberg MJ (2000) Enhanced genome annotation using structural profiles in the program 3D-PSSM. J Mol Biol **299:** 499–520

Kim JY (2005) Regulation of short-distance transport of RNA and protein. Curr Opin Plant Biol **8:** 45–52

King RW, Zeevaart JA (1974) Enhancement of phloem exudation from cut petioles by chelating agents. Plant Physiol **53:** 96–103

Knoblauch M, Noll GA, Muller T, Prufer D, Schneider-Huther I, Scharner D, Van Bel AJ, Peters WS (2003) ATP-independent contractile proteins from plants. Nat Mater **2:** 600–603

Knoblauch M, Peters WS, Ehlers K, van Bel AJ (2001) Reversible calcium-regulated stopcocks in legume sieve tubes. Plant Cell **13:** 1221–1230

Labesse G, Mornon J (1998) Incremental threading optimization (TITO) to help alignment and modelling of remote homologues. Bioinformatics **14:** 206–211

Laemmli UK (1970) Cleavage of structural proteins during the assembly of the head of bacteriophage T4. Nature **227:** 680–685

Le Hir R, Beneteau J, Bellini C, Vilaine F, Dinant S (2008) Gene expression profiling: keys for investigating phloem functions. Trends Plant Sci **13:** 273–280

Lee JY, Yoo BC, Rojas MR, Gomez-Ospina N, Staehelin LA, Lucas WJ (2003) Selective trafficking of non-cell-autonomous proteins mediated by NtNCAPP1. Science **299:** 392–396

Lehmann F, Tiralongo E, Tiralongo J (2006) Sialic acid-specific lectins: occurrence, specificity and function. Cell Mol Life Sci **63:** 1331–1354

Leineweber K, Schulz A, Thompson GA (2000) Dynamic transitions in the translocated phloem filament protein. Aust J Plant Physiol **27:** 733–741

Lerouge P, Cabanes-Macheteau M, Rayon C, Fischette-Laine AC, Gomord V, Faye L (1998) N-Glycoprotein biosynthesis in plants: recent developments and future trends. Plant Mol Biol **38:** 31–48

Lin MK, Lee YJ, Lough TJ, Phinney BS, Lucas WJ (2009) Analysis of the

pumpkin phloem proteome provides insights into angiosperm sieve tube function. Mol Cell Proteomics **8:** 343–356

Lough TJ, Lucas WJ (2006) Integrative plant biology: role of phloem long-distance macromolecular trafficking. Annu Rev Plant Biol **57:** 203–232

Lucas WJ, Lee JY (2004) Plasmodesmata as a supracellular control network in plants. Nat Rev Mol Cell Biol **5:** 712–726

Mustroph A, Zanetti ME, Jang CJH, Holtan HE, Repetti PP, Galbraith DW, Girke T, Bailey-Serres J (2009) Profiling translatomes of discrete cell populations resolves altered cellular priorities during hypoxia in Arabidopsis. Proc Natl Acad Sci USA **106:** 18843–18848

Noll GA, Fontanellaz ME, Ruping B, Ashoub A, van Bel AJ, Fischer R, Knoblauch M, Prufer D (2007) Spatial and temporal regulation of the forisome gene *for1* in the phloem during plant development. Plant Mol Biol **65:** 285–294

Oparka KJ, Cruz SS (2000) The great escape: phloem transport and unloading of macromolecules. Annu Rev Plant Physiol Plant Mol Biol **51:** 323–347

Owens RA, Blackburn M, Ding B (2001) Possible involvement of the phloem lectin in long-distance viroid movement. Mol Plant Microbe Interact **14:** 905–909

Pelissier HC, Peters WS, Collier R, van Bel AJ, Knoblauch M (2008) GFP tagging of sieve element occlusion (SEO) proteins results in green fluorescent forisomes. Plant Cell Physiol **49:** 1699–1710

Peumans WJ, Van Damme EJ (1995) Lectins as plant defense proteins. Plant Physiol **109:** 347–352

Rahbé Y, Febvay G (1993) Protein toxicity to aphids: an in vitro test on *Acyrthosiphon pisum*. Entomol Exp Appl **67:** 149–160

Read SM, Northcote DH (1983a) Subunit structure and interactions of the phloem proteins of *Cucurbita maxima* (pumpkin). Eur J Biochem **134:** 561–569

Read SM, Northcote DH (1983b) Chemical and immunological similarities between the phloem proteins of three genera of the Cucurbitaceae. Planta **158:** 119–127

Renard D, Lefebvre J, Griffin MC, Griffin WG (1998) Effects of pH and salt environment on the association of beta-lactoglobulin revealed by intrinsic fluorescence studies. Int J Biol Macromol **22:** 41–49

Richardson P, Baker D, Ho L (1982) The chemical composition of cucurbit vascular exudates. J Exp Bot **33:** 1239–1247

Sabnis DD, Hart JW (1978) The isolation and some properties of a lectin (haemagglutinin) from *Cucurbita* phloem exudate. Planta **142:** 97–101

Sauvion N, Charles H, Febvay G, Rahbé Y (2004) Effects of jackbean lectin (ConA) on the feeding behaviour and kinetics of intoxication of the pea aphid, *Acyrthosiphon pisum*. Entomol Exp Appl **110:** 31–44

Scatchard G (1949) The attractions of proteins for small molecules and ions. Ann N Y Acad Sci **51:** 660–672

Schauer R (2009) Sialic acids as regulators of molecular and cellular interactions. Curr Opin Struct Biol **19:** 507–514

Schrader J, Nilsson J, Mellerowicz E, Berglund A, Nilsson P, Hertzberg M, Sandberg G (2004) A high-resolution transcript profile across the wood-forming meristem of poplar identifies potential regulators of cambial stem cell identity. Plant Cell **16:** 2278–2292

Scott CL, Hartweck LM, de Jesus Perez J, Chen D, Garcia JA, Olszewski NE (2006) SECRET AGENT, an *Arabidopsis thaliana* O-GlcNAc transferase, modifies the plum pox virus capsid protein. FEBS Lett **580:** 5829–5835

Sigrist CJ, Cerutti L, Hulo N, Gattiker A, Falquet L, Pagni M, Bairoch A, Bucher P (2002) PROSITE: a documented database using patterns and profiles as motif descriptors. Brief Bioinform **3:** 265–274

Sjölund RD (1997) The phloem sieve element: a river runs through it. Plant Cell **9:** 1137–1146

Smith LM, Sabnis DD, Johnson RPC (1987) Immunocytochemical localisation of phloem lectin from *Cucurbita maxima* using peroxidase and colloidal-gold labels. Planta **170:** 461–470

Spanner DC (1978) Sieve-plate pores, open or occluded? A critical review. Plant Cell Environ **1:** 7–20

Strasser R, Altmann F, Glossl J, Steinkellner H (2004) Unaltered complex N-glycan profiles in *Nicotiana benthamiana* despite drastic reduction of beta1,2-N-acetylglucosaminyltransferase I activity. Glycoconj J **21:** 275–282

Strasser R, Stadlmann J, Svoboda B, Altmann F, Glossl J, Mach L (2005) Molecular basis of N-acetylglucosaminyltransferase I deficiency in *Arabidopsis thaliana* plants lacking complex N-glycans. Biochem J **387:** 385–391

Subramanyam S, Smith DF, Clemens JC, Webb MA, Sardesai N, Williams CE (2008) Functional characterization of HFR1, a high-mannose N-glycan-specific wheat lectin induced by Hessian fly larvae. Plant Physiol **147:** 1412–1426

Suzui N, Nakamura S-i, Fujiwara T, Hayashi H, Yoneyama T (2006) A putative acyl-CoA-binding protein is a major phloem sap protein in rice (*Oryza sativa* L.). J Exp Bot **57:** 2571–2576

Taoka K, Ham BK, Xoconostle-Cazares B, Rojas MR, Lucas WJ (2007) Reciprocal phosphorylation and glycosylation recognition motifs control NCAPP1 interaction with pumpkin phloem proteins and their cell-to-cell movement. Plant Cell **19:** 1866–1884

Thompson GA, Schulz A (1999) Macromolecular trafficking in the phloem. Trends Plant Sci **4:** 354–360

Tomiya N, Narang S, Lee YC, Betenbaugh MJ (2004) Comparing N-glycan processing in mammalian cell lines to native and engineered lepidopteran insect cell lines. Glycoconj J **21:** 343–360

Turgeon R, Wolf S (2009) Phloem transport: cellular pathways and molecular trafficking. Annu Rev Plant Biol **60:** 207–221

Van Bel AJE (2003) The phloem, a miracle of ingenuity. Plant Cell Environ **26:** 125–149

van Bel AJE, Gaupels F (2004) Pathogen-induced resistance and alarm signals in the phloem. Mol Plant Pathol **5:** 495–504

Van Damme EJ, Barre A, Rouge P, Peumans WJ (2004) Cytoplasmic/nuclear plant lectins: a new story. Trends Plant Sci **9:** 484–489

Vasconcelos IM, Oliveira JT (2004) Antinutritional properties of plant lectins. Toxicon **44:** 385–403

Verwoerd TC, Dekker BM, Hoekema A (1989) A small-scale procedure for the rapid isolation of plant RNAs. Nucleic Acids Res **17:** 2362

Vilaine F, Palauqui JC, Amselem J, Kusiak C, Lemoine R, Dinant S (2003) Towards deciphering phloem: a transcriptome analysis of the phloem of *Apium graveolens*. Plant J **36:** 67–81

Vimr E, Lichtensteiger C (2002) To sialylate, or not to sialylate: that is the question. Trends Microbiol **10:** 254–257

von Grotthuss M, Pas J, Wyrwicz L, Ginalski K, Rychlewski L (2003) Application of 3D-Jury, GRDB, and Verify3D in fold recognition. Proteins **53:** 418–423

Walz C, Giavalisco P, Schad M, Juenger M, Klose J, Kehr J (2004) Proteomics of curcurbit phloem exudate reveals a network of defence proteins. Phytochemistry **65:** 1795–1804

Walz C, Juenger M, Schad M, Kehr J (2002) Evidence for the presence and activity of a complete antioxidant defence system in mature sieve tubes. Plant J **31:** 189–197

Wells L, Hart GW (2003) O-GlcNAc turns twenty: functional implications for post-translational modification of nuclear and cytosolic proteins with a sugar. FEBS Lett **546:** 154–158

Xie H, Gilbert HJ, Charnock SJ, Davies GJ, Williamson MP, Simpson PJ, Raghothama S, Fontes CM, Dias FM, Ferreira LM, et al (2001) *Clostridium thermocellum* Xyn10B carbohydrate-binding module 22-2: the role of conserved amino acids in ligand binding. Biochemistry **40:** 9167–9176

Zeleny R, Kolarich D, Strasser R, Altmann F (2006) Sialic acid concentrations in plants are in the range of inadvertent contamination. Planta **224:** 222–227

Zhao C, Craig JC, Petzold HE, Dickerman AW, Beers EP (2005) The xylem and phloem transcriptomes from secondary tissues of the Arabidopsis root hypocotyl. Plant Physiol **138:** 803–818